© 2019. Published by The Company of Biologists Ltd | Development (2019) 146, dev177709. doi:10.1242/dev.177709

REVIEW

Positional information and tissue scaling during development and regeneration

Daniel Čapek[1] and Patrick Müller[1,2,*]

ABSTRACT

In order to contribute to the appropriate tissues during development, cells need to know their position within the embryo. This positional information is conveyed by gradients of signaling molecules, termed morphogens, that are produced in specific regions of the embryo and induce concentration-dependent responses in target tissues. Positional information is remarkably robust, and embryos often develop with the correct proportions even if large parts of the embryo are removed. In this Review, we discuss classical embryological experiments and modern quantitative analyses that have led to mechanistic insights into how morphogen gradients adapt, scale and properly pattern differently sized domains. We analyze these experimental findings in the context of mathematical models and synthesize general principles that apply to multiple systems across species and developmental stages.

KEY WORDS: French Flag model, Morphogens, Pattern formation, Positional information, Regeneration, Scaling

Introduction

In his celebrated 1969 paper, Lewis Wolpert stated that 'The effective distinguishing feature between mosaic and regulative development is that when a portion of the system is removed, then the mosaic system will largely lack those regions which the removed portion would normally form, whereas in regulative systems a normal pattern would still be formed. I have formalized the problem of the regulative development of axial patterns, whose pattern is size invariant, in terms of the French Flag problem' (Wolpert, 1969). This statement forms the essence of Wolpert's paper: what is the minimal model that can explain how a pattern forms during development, how does it regulate tissue proportions in differently sized embryos, and how does it lead to regeneration if large portions of tissue are removed from an adult organism? The minimal model that emerged is the famous gradient-based model (often referred to as the 'French Flag model') that Wolpert postulated in an earlier paper (Wolpert, 1968): a signaling gradient (e.g. of a diffusible molecule) along a one-dimensional field of elements (e.g. cells) is read out at fixed concentration thresholds that give rise to three different tissue types – in case of the French flag, blue, white and red ones (Fig. 1A).

The idea that gradients underlie patterning had already been expressed in the early 20th century (Boveri, 1901; Morgan, 1901). Subsequently, thresholds were postulated (Dalq, 1938) and Turing coined the term 'morphogens' to define molecules responsible for pattern formation (Turing, 1952). Experimental evidence to support the concept that cell fates are induced by gradients of morphogens from signaling centers was provided in the 1960s from transplantation and ablation experiments in moths and leafhoppers (Sander, 1959; Stumpf, 1966). This led to the idea that each cell can be assigned a positional value relative to a signaling center (Lawrence, 1966; Rogers and Schier, 2011; Stumpf, 1966; Wolpert, 1968, 1969).

If in such a scenario the gradients or thresholds do not change concomitantly with tissue size, incorrect tissue proportions should arise (Fig. 1B,C). However, this is not observed in the vast majority of embryos analyzed so far. Instead there are numerous examples from development and regeneration throughout the animal kingdom of proper patterning in differently sized individuals. This raises the intriguing issue of how signaling gradients scale in order to give rise to the correct tissue dimensions. Patterning mechanisms must not only convey positional information, but they also have to be robust against changes in the size of the patterning field.

In this Review, we discuss mechanisms that provide size invariance of patterning systems. We focus on scaling systems during animal development, when positional information is established *de novo*, and in adult regeneration, when positional information must be re-established and reconnected to the polarity of existing structures. We highlight mathematical models that describe scaling, illustrate mechanisms that allow the scaling of morphogen gradients and provide examples of experimental data supporting these concepts.

Classical embryological experiments

To provide historical context for our analyses, we first provide an overview of classical experiments with sea urchins, Hydra, fish and amphibians that have demonstrated that correct tissue proportions can be established even when the overall size of an organism is dramatically reduced after surgical manipulation (Cooke, 1975; Driesch, 1892; Hoadley, 1928; Holtfreter, 1938; Mangold, 1960; Morgan, 1895; Nicholas and Oppenheimer, 1942; Sander, 1959; Spemann, 1938; Wolpert, 1969).

The issue of how robust development is towards size manipulation arose in the late 19th century, originally as a tangent to the debate on preformationism. In his *Princip der organbildenden Keimbezirke*, Wilhelm His proposed that the germ disc of chicken embryos contains the primordia for all organs as flat projections and that, vice versa, each position on the germ disc corresponds to a specific position in a later organ (His, 1874). To investigate this hypothesis, Wilhelm Roux performed experiments in which he killed one blastomere of amphibian embryos at the two-cell stage with a hot needle (Box 1) (Roux, 1885). He found that this treatment led to the development of half embryos – embryos in which the body parts that would have been formed by the killed blastomere are missing – that he dubbed 'Halbbildungen'. This was interpreted as a confirmation

[1]Systems Biology of Development Group, Friedrich Miescher Laboratory of the Max Planck Society, Max-Planck-Ring 9, 72076 Tübingen Germany. [2]Modeling Tumorigenesis Group, Translational Oncology Division, Eberhard Karls University Tübingen, Otfried-Müller-Strasse 10, 72076 Tübingen Germany.

*Author for correspondence (patrick.mueller@tuebingen.mpg.de)

D.Č., 0000-0001-5199-9940; P.M., 0000-0002-0702-6209

Development (2019) 146, dev177709. doi:10.1242/dev.177709

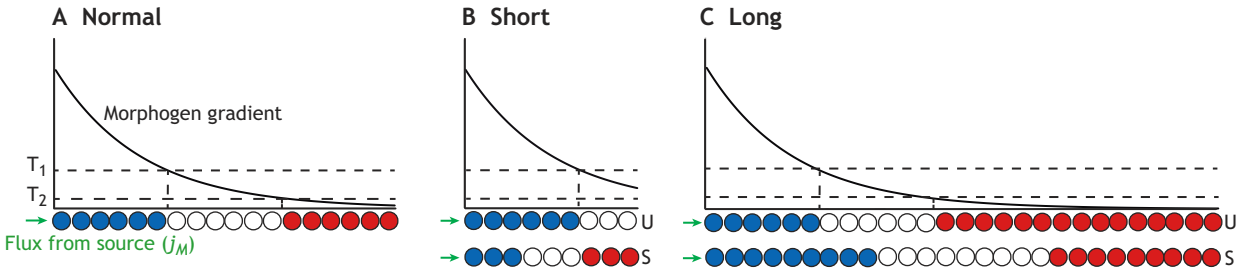

Fig. 1. Positional information and morphogens. Schematic of the French Flag problem. (A) A field of tissue is patterned by a morphogen gradient based on two thresholds (T_1 and T_2) into three distinct cell fates – in this case blue, white and red. The green arrows show the flux (j_M) of morphogen from the source. (B,C) If the size of the tissue is decreased (B) or increased (C) and the gradient is unchanged, patterns with the wrong proportions are formed, i.e. they are 'unscaled' (U). However, in most cases, embryonic tissues adjust to changes in size and display correctly scaled (S) pattern proportions.

of the preformationism theory, as half embryos could not establish their full body plan.

Roux's results were later challenged by Hans Driesch, who separated blastomeres of sea urchin embryos through shaking and found that these embryos developed into intact smaller versions ('Theilbildungen') of their untreated siblings, contradicting Roux's results (Driesch, 1892). Based on these and the earlier findings of Chabry (1887) and the Hertwig brothers (Hertwig, 1890; Hertwig and Hertwig, 1887), Driesch concluded that embryos are not predetermined. However, he did not comment on potential mechanisms underlying the observed scale-invariant patterning.

When Thomas Hunt Morgan re-examined the results of Hertwig and Roux, he found that both datasets also contained cases of the other, i.e. Hertwig also obtained a small proportion of Halbbildungen and Roux's method generated some size-reduced whole embryos (Hertwig, 1893; Morgan, 1895; Roux, 1894). When Morgan repeated the experiments on frog embryos, he likewise found both types of experimental outcomes. Eventually, the outcome of these experiments turned out to depend on an additional factor, namely whether the killed cell was removed or not (Bruns, 1931; Vogt and Bruns, 1930). Morgan eventually determined that scaling must take place in those instances in which viable adults developed: 'Readjustments to the size of the mass must take place because the embryo that emerges is not the anterior half of an embryo but a whole embryo of half size' (Morgan, 1924).

An increasing number of examples of embryos that can form perfectly scaled, albeit smaller, individuals after the separation of blastomeres was subsequently found across different species, e.g. lancelets and newt (Morgan, 1896; Wilson, 1893). Moreover, experiments by Mangold and Spemann as well as Holtfreter showed more specifically that individual structures can scale with embryo size and that substructures, such as the lateral part (Seitenkappe) of an amphibian gastrula, can give rise to a full bilateral embryo (Holtfreter, 1938; Ruud and Spemann, 1922; Spemann and Mangold, 1924). However, the discussion still revolved around the problem of preformation rather than how scale invariance is achieved.

The question regarding the molecular mechanisms of scale-invariant patterning only moved into the spotlight with the introduction of mathematical models of development, most notably Wolpert's gradient model described above, and Turing's and Gierer and Meinhardt's reaction-diffusion (RD) systems (Gierer and Meinhardt, 1972; Turing, 1952; Wolpert, 1968, 1969). These RD systems are based on two diffusible components. One molecule, termed the 'activator', positively feeds back on its own synthesis and at the same time activates the other component (Gierer and Meinhardt, 1972). The other molecule is termed the 'inhibitor' because it negatively regulates itself and the activator. Indeed, it has since been shown that interactions between diffusible activators and inhibitors can amplify small random fluctuations, leading to self-organized repeated wave-like patterns of signaling that can be translated into periodic morphological elements (Landge et al., 2019).

Although both the gradient and RD models can explain many instances of patterning, it became clear that they are not sufficient to fully account for scale-invariant development. In 1975, Cooke counted the somites of surgically size-reduced *Xenopus* embryos and found that somite size, but not somite number, was changed (Cooke, 1975). He pointed out that a Turing-type RD system should give the opposite outcome, unless the physiochemical properties of the involved molecules, such as their diffusivities, are changed. Pure positional information models, on the other hand, would not easily give rise to repeated elements. He subsequently developed the clock-wavefront model of somitogenesis, which incorporated a scale-invariant gradient of positional information and a cellular oscillator for generating repeated elements (Cooke and Zeeman, 1976).

It also became clear that there are limits to the scaling capacity of embryos. As mentioned above, embryos do not always downscale and compensate if the dead cell is not removed (Bruns, 1931; Vogt and Bruns, 1930). Likewise, the time window during which an organism can adjust to achieve normal patterning can be limited. For example, Klaus Sander's Schnürungs experiments, in which he divided embryos of the leafhopper *Euscelis* using a nylon loop (Box 1), revealed that scaling is not only dependent on the position of missing body parts but also depends on the developmental stage during which the procedure is performed (Sander, 1959). Similarly, manipulated amphibian gastrulae can form complete body plans, whereas surgery at later neurula stages results in missing body parts (Mangold, 1960). Finally, although it remains unclear how widespread scaling actually is, it is likely that most animals with a regulative mode of embryogenesis possess the ability to scale tissue proportions to some extent (while organisms that exhibit mosaic development, such as nematodes, cannot compensate for the loss of blastomeres).

Scaling models

In order for scaling to occur, information about tissue size must be encoded in some aspect of the patterning system. Below, we outline the mathematics and underlying concepts of four major experimentally supported scale-invariant patterning models.

Scaling by specific boundary conditions

In his original 1968 paper on the French Flag problem, Wolpert suggested that linear gradients can scale if the concentration of morphogen at the source and sink remains fixed at a constant level

Development (2019) 146, dev177709. doi:10.1242/dev.177709

Box 1. Experimental embryology: size reduction methods

Overview of classical and recent embryological methods that have been used for surgical size reduction. (A-D) Methods of surgical manipulation in amphibian embryos. The first approach in experimental embryology involved the destruction of one blastomere at the two-cell stage using a hot needle (A) (Roux, 1894). If the killed blastomere remains attached, a half embryo is formed. If the two blastomeres are lassoed (B) using, for example, baby hair (Spemann, 1903) in the plane of the first cleavage, both parts develop smaller but properly patterned embryos with correct tissue proportions. Likewise, sagittal sectioning with an eyelash at mid-blastula stages leads to twin development (C) (Moriyama and De Robertis, 2018). (D) Schematic of the Spemann-Mangold organizer experiment in which a part of organizer tissue was removed with tungsten wire and forceps (Spemann and Mangold, 1924). (E) Schematic of Klaus Sander's *Euscelis* experiments in which eggs were lassoed at various anterior-posterior positions and stages with a nylon fiber (Sander, 1959). (F-H) Methods for size reduction in pre-gastrulation zebrafish embryos. (F) Up to 30% of cells can be removed from the animal pole by extirpation with a glass capillary connected to a syringe (Almuedo-Castillo et al., 2018). (G) Alternatively, the animal pole blastoderm can be cut off with a glass pipette or a steel wire; the yolk is simultaneously wounded to achieve symmetric size reduction (Ishimatsu et al., 2019, 2018). (H) A third approach uses a tungsten needle to injure the yolk, thereby achieving size reduction exclusively via yolk removal (Huang and Umulis, 2019).

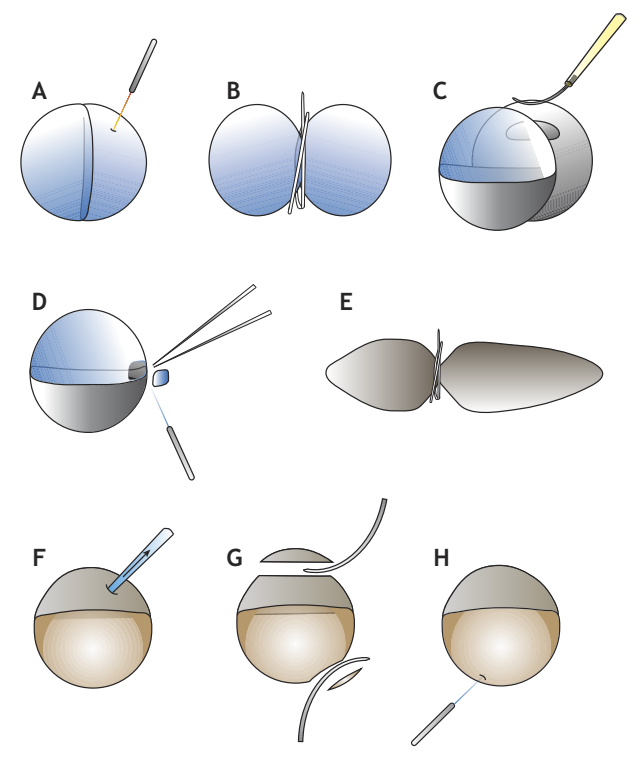

(Fig. 2A, top panel) (Wolpert, 1968). However, the plausibility of this tenet and the mechanisms underlying the formation of relevant gradients were unknown. Two years later, Francis Crick suggested a simple one-dimensional gradient model with a morphogen diffusing from a localized source on one side of the patterning field and a sink on the other side as boundary conditions (Crick, 1970). The source produces the morphogen and maintains it at a stable level, whereas the sink destroys morphogen molecules that reach it to a fixed level. In mathematical terms, the change in the concentration of a morphogen molecule M as a function of time t in this system can be described as:

$$\frac{\partial M}{\partial t} = D_M \nabla^2 M,$$

in which the Laplace operator ∇^2 describes the divergence of the gradient. The morphogen molecules spread with a diffusion coefficient D_M. Their level at the source at the position x=0 (i.e. at one end of the field) is held constant at a concentration of $M(x=0)=M_0$, and their level at the sink at position $x=L$ (i.e. the other end of the field) is $M(x=L)=0$. Once the gradient reaches a steady state, the concentration values at all positions x no longer change. The steady-state solution of this system as a function of space x is:

$$M(x) = M_0\left(1 - \frac{x}{L}\right).$$

This equation demonstrates perfect scaling of the gradient that was generated by this mechanism, as the spatial profile of the morphogen M is a function of relative position x/L rather than x alone (Ben-Zvi and Barkai, 2010). Crick found that relevant gradients in tissues using this mechanism could form over biologically realistic time scales, demonstrating the plausibility of a gradient formation mechanism (Crick, 1970). However, how the morphogen concentration at the ends of the field could be held constant, as postulated by Wolpert, remained unresolved.

There is now strong evidence to show that many morphogen gradients form via production from a localized source combined with morphogen diffusion and uniform degradation throughout an embryonic field (reviewed by Müller et al., 2013; Rogers and Müller, 2019). This so-called synthesis-diffusion-degradation (SDD) model can be formalized by the following differential equation:

$$\frac{\partial M}{\partial t} = D_M \nabla^2 M - k_M M.$$

This describes the time-dependent change in the concentration of the morphogen molecule M that is produced in a localized source at the boundary with a flux j_M (Fig. 2A, bottom panel). The morphogen spreads with a diffusion coefficient D_M, and its degradation is governed by the degradation constant k_M. Assuming a model in which the patterning field is continuous, the degradation rate is linear (i.e. the degradation rate does not depend on morphogen concentration) and the morphogen range [defined as the position at which the concentration $M(x)$ falls below the detection level] is smaller than the patterning field, the steady-state gradient of M can be described as an exponential function (reviewed by Bollenbach et al., 2007; Wartlick et al., 2009):

$$M(x) = M_0 e^{-\frac{x}{\lambda}}$$

in which M_0 is the concentration at the source and λ is the characteristic decay length of the gradient. M_0 is a function of production, degradation and diffusion:

$$M_0 = \frac{j_M}{\sqrt{D_M k_M}}.$$

If the size of the source is changed in differently sized embryos, this would automatically change the production term j_M. For example, a smaller source would provide a smaller flux j_M, whereas a larger source would provide a higher flux j_M. This change in the flux would change the amplitude and the range (Fig. 2A, bottom panel), but it does not yield perfect scaling of the morphogen gradient at all positions of the patterning field (Umulis and Othmer,

Development (2019) 146, dev177709. doi:10.1242/dev.177709

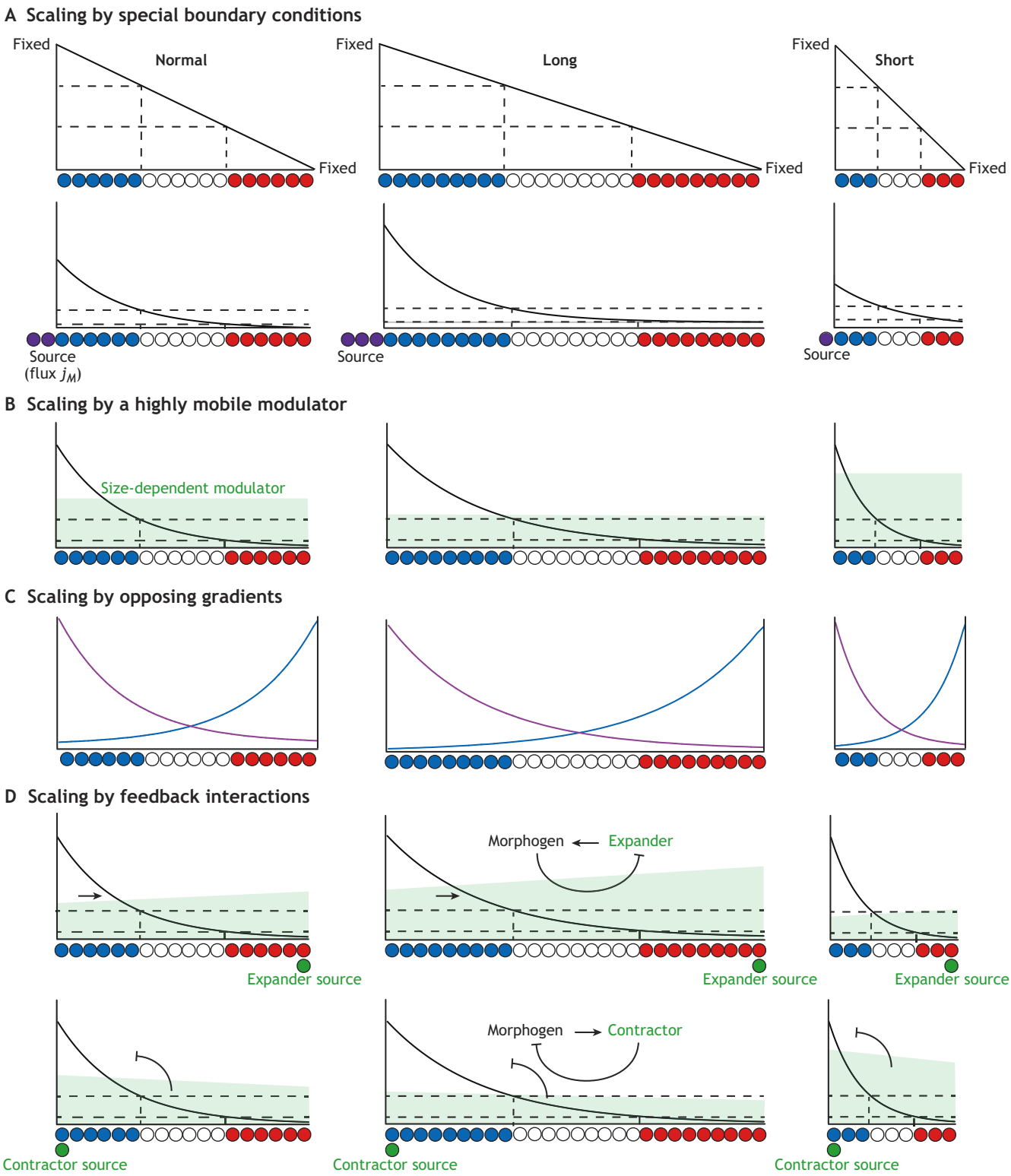

Fig. 2. Four major models of scale-invariant patterning. (A) Gradients can scale by adjusting boundary conditions. A simple method of gradient scaling involves fixed morphogen concentrations at both ends of the field (upper panel) (Crick, 1970; Wolpert, 1968, 1969). Another option is up- or downregulation of morphogen production by source cells (lower panel, up or downregulation shown by increased or decreased source size; purple cells) (Cheung et al., 2011; He et al., 2008). (B) Gradients can also scale through modulation by a diffusible molecule. The field size is measured by a modulator (green) of the diffusion or degradation properties of the morphogen. If the modulator concentration decreases in a larger field, the morphogen range is increased. If the modulator concentration rises in a smaller field, the morphogen range shrinks. (C) Scaling can also be achieved if cells read out the ratio between opposing gradients (purple and blue) and thus adjust their positional information. (D) Feedback interactions can also contribute to scaling. In the expansion-repression model (upper panel), an expander molecule whose expression is repressed by the morphogen facilitates diffusion of the morphogen. This negative feedback limits the amount of available expander and therefore the shape of the gradient. In the induction-contraction model (lower panel), diffusion and gradient range are negatively regulated by a target of the morphogen: the contractor.

Development (2019) 146, dev177709. doi:10.1242/dev.177709

2013). However, this approximate scaling is likely sufficient in many contexts, especially if the gradient provides a rough pre-pattern that is later refined by other patterning systems.

Therefore, a simple mechanism for adjusting a gradient to a new size is to invoke a change in the boundary conditions. In this model, if the target tissue width becomes reduced, the production rate must decrease accordingly in order to maintain the relative shape of the gradient. If, on the other hand, the tissue grows, the production must increase to match the wider patterning field (Fig. 2A).

Scaling by adjusting degradation or diffusion with a highly mobile modulator

The characteristic decay length λ of the exponential morphogen gradient described above is a direct measure of the gradient's range. Importantly, the decay length λ is a function of both the diffusion coefficient D_M and the degradation constant k_M:

$$\lambda = \sqrt{\frac{D_M}{k_M}}.$$

This relationship between λ, D_M and k_M implies that the range of a gradient could be adjusted by changing the diffusion coefficient D_M or the degradation constant k_M of the morphogen. Therefore, a good strategy to achieve scale invariance is to couple these two biophysical properties to field size. From first principles, however, it is difficult to conceive how the biophysical properties of a morphogen could be influenced by a change in the size of the patterning field. According to the Einstein-Stokes relation, the diffusion coefficient D_M depends on the size of the morphogen, the viscosity of the medium in which it diffuses and the surrounding temperature (reviewed in Müller and Schier, 2011). All of these properties should in principal be unaffected in differently sized patterning fields, and therefore the diffusion coefficient would remain unchanged.

To solve this conundrum, it has been proposed that the biophysical properties of a morphogen can be influenced by accessory modulator molecules that sense tissue size (Rasolonjanahary and Vasiev, 2016, 2018). In this context, the general differential equation describing morphogen gradient formation can be extended by incorporating a modulator molecule S produced with a localized flux j_S that affects the degradation rate of the morphogen M:

$$\frac{\partial M}{\partial t} = D_M \nabla^2 M - k_M M S^n$$

and

$$\frac{\partial S}{\partial t} = D_S \nabla^2 S - k_S S,$$

where n indicates the strength of the modulator degrading the morphogen. It is important to note that 'degradation' in this context does not only refer to physical destruction, but to any clearance mechanism that results in the effective removal of the morphogen from the patterning system (e.g. irreversible complex formation, etc.). In the simple case of a hypothetical decay strength n=2, the steady-state solution for the morphogen gradient is

$$M(x) = M_0 e^{-\frac{x}{L}\left(\frac{D_S j_S}{k_S}\sqrt{\frac{k_M}{D_M}}\right)}.$$

This equation shows perfect scaling of the morphogen gradient, as the spatial profile of M is a function of relative position x/L rather than x alone (i.e. as seen in the simple system without a modulator described above). In this model, the modulator needs to have a high diffusivity D_s, so that it can relay information about field size based on its accumulation in smaller domains or dilution in larger domains. In smaller embryos, the concentration of the highly diffusible inhibitor would rise (Fig. 2B) and therefore shrink the range of the morphogen. In larger embryos, the inhibitor would be more diluted because of its high diffusivity, allowing the morphogen to disperse over a wider region (Fig. 2B).

Modulator molecules whose expression is independent of the morphogen have been called passive modulators, whereas modulators whose expression is strongly connected to morphogen concentration have been called active modulators (Umulis and Othmer, 2013). Conceptually similar models with different boundary conditions that lead to self-organized and size-independent pattern formation include wave pinning (Ishihara and Tanaka, 2018; Mori et al., 2008) and models with saturation of autocatalysis (Gierer and Meinhardt, 1972). Related models in which morphogen diffusivities are proportional to field size have also been proposed (Othmer and Pate, 1980; Pate and Othmer, 1984).

Scaling by opposing gradients

Interactions between two morphogen gradients emerging from opposite ends of a patterning field can also result in scale-invariant patterning (McHale et al., 2006). This possibility had already been considered by Wolpert in 1969 for the ratiometric readout of vegetal and animal gradients in sea urchins (Fig. 2C) (Wolpert, 1969). Consider two morphogens, M and O, emerging from opposite ends of the embryonic field:

$$\frac{\partial M}{\partial t} = D_M \nabla^2 M - k_M M$$

with flux from one end of the field, x=0, and

$$\frac{\partial O}{\partial t} = D_M \nabla^2 O - k_M O$$

with flux from the other end of the field, x=L. The model assumes the same diffusivities and degradation rates for both molecules, and thus the two gradients will have the same steady-state distribution, but with opposite polarities (Fig. 2C):

$$M(x) = M_0 e^{-\frac{x}{\lambda_M}}$$

and

$$O(x) = M_0 e^{\frac{x-L}{\lambda_M}}.$$

For morphogen-dependent target genes that are activated whenever $M(x)$ is larger than $O(x)$, the expression boundary can be found at:

$$x_b = \frac{L}{2}.$$

Thus, gradients formed and interpreted in this manner are read out exactly in the middle of the embryo and automatically scale with the field size L (Houchmandzadeh et al., 2005). This mechanism can be extended to systems in which the biophysical properties and resulting spatial ranges λ_M and λ_O of the opposing morphogens differ (Houchmandzadeh et al., 2005), and the resulting scale-invariant readout is:

$$x_b = \frac{\lambda_M L}{\lambda_M + \lambda_O}.$$

This mechanism based on two opposing morphogen gradients works well to scale the boundaries of individual target genes, but it

Development (2019) 146, dev177709. doi:10.1242/dev.177709

only poorly accounts for the scaling of multiple morphogen-dependent responses with different activation thresholds, as the readout gradient does not scale well across the entire field (McHale et al., 2006). The degree of scaling for opposing gradient-based mechanisms can be improved when the molecules are irreversibly inactivated upon binding to each other (McHale et al., 2006).

Scaling by feedback interactions

Patterning systems that convey the largest degree of scaling across the entire embryonic field incorporate feedback interactions between the morphogen and modulator molecules. As mentioned above, these feedback-dependent molecules are referred to as active modulators (Umulis and Othmer, 2013). The most prominent model of these is the 'expansion-repression' mechanism (Fig. 2D, top panel) (Ben-Zvi and Barkai, 2010), which has found experimental support from fruit flies to zebrafish (discussed below). The fundamental tenet of this model is that morphogen range can be increased by an expander molecule, which changes the diffusion or degradation properties of the morphogen. In turn, the expression of the expander is negatively regulated by the morphogen. The gradient formation dynamics in this system can be described by:

$$\frac{\partial M}{\partial t} = D_M \nabla^2 M - k_M(E) M \quad \text{or} \quad \frac{\partial M}{\partial t} = D_M(E) \nabla^2 M - k_M M,$$

with a localized morphogen flux j_M from one end of the field. Importantly, in this model the diffusion coefficient D_M or the degradation constant k_M of the morphogen is dependent on the level of an expander molecule E produced on the side that is opposite to the morphogen source. The gradient formation dynamics of the expander molecule, in turn, are controlled by the morphogen M:

$$\frac{\partial E}{\partial t} = D_E \nabla^2 E - k_E E + \sigma \frac{T}{T + M}.$$

Here, the morphogen M inhibits the production of the expander molecule E depending on the repression threshold T (the rate constant σ regulates the production levels). Importantly, the expander molecule needs to have a high diffusivity D_E and must be stable in order to rapidly equilibrate across the field and therefore relay information about field size. The steady-state morphogen profile fulfills the relationship:

$$M(x) = M_0\left(\frac{x}{L}, \frac{j_M \lambda}{D_M}\right),$$

which shows that the morphogen gradient scales as a function of the field size L (Ben-Zvi and Barkai, 2010). In this mechanism, expander molecules initially increase the range of the morphogen until the morphogen levels are high enough to halt the expression of the expander, which in turn ends the spatial expansion of the morphogen gradient. In a larger tissue, morphogen levels on the opposing side of the source are initially not as high as those in normally sized tissues. Morphogen expression and range expansion thus continue until a critical threshold for expander repression is reached. This mechanism therefore establishes perfect scaling by increasing morphogen range in larger tissues and, analogously, decreasing it in smaller tissues.

Interestingly, the mirror-symmetric 'induction-contraction' model – in which a contractor molecule is activated by the morphogen and contracts its range – also scales (Fig. 2D, bottom panel) (Rahimi et al., 2016), and similar principles can even be applied to self-organizing pattern formation systems that lack initial polarity (Werner et al., 2015). Finally, feedback between tissue mechanics and morphogen turnover or transport can also lead to size-invariant scaling in advection-driven self-organizing models, even with a single morphogen species (Recho et al., 2019).

In summary, tissues that depend on precise morphogen gradients need to adjust the length scale of morphogen distribution to the size of the tissue, which can be achieved by special boundary conditions, opposing gradients and modulators affecting the mobility or stability of the morphogen. It is possible that different strategies or combinations of strategies are used in different developmental contexts, and it is therefore necessary to perform experimental measurements for model validation. Finally, it will be important to extend future theoretical models to take into account the noise and variability that is often observed in patterning systems.

Molecular insights into scaling mechanisms

Owing to advances in molecular biology, imaging, genomics and computational biology, the last 15 years have seen a surge of scaling studies that have uncovered some of the mechanisms underlying the observations of classical experimental embryology described above. Below, we highlight recent studies that have used modern molecular biology methods to identify new principles controlling scale-invariant patterning during embryogenesis and regeneration. We analyze these findings in the context of the concepts and mathematical models introduced above.

Scaling during embryonic development

Numerous experiments have demonstrated the existence of mechanisms that allow embryonic axes and tissues to scale during development. For example, surgically reducing the size of developing zebrafish embryos by 30% (Box 1) typically results in normally patterned, viable larvae and adults (Almuedo-Castillo et al., 2018; Collins et al., 2019 preprint; Huang and Umulis, 2019; Ishimatsu et al., 2019, 2018). Even more drastically, amphibian half embryos (Box 1) that originate from either the lateral (Moriyama and De Robertis, 2018; Reversade and De Robertis, 2005) or dorsal half (Spemann, 1903) form properly patterned miniature organisms. Here, we focus on some well-studied vertebrate systems and synthesize the mechanisms that can explain classical embryological experiments, from Spemann's early dorsal-ventral patterning experiments to Cooke's somite scaling observations. Excellent progress has also been made in invertebrate systems, as reviewed previously (Umulis and Othmer, 2013).

Scaling of dorsal-ventral patterning

The dorsal-ventral (DV) axis of vertebrate embryos is patterned by a gradient of bone morphogenetic proteins (BMPs) that activate the phosphorylation of the transcriptional effector Smad1/5/9 (pSmad1/5/9) via heterodimeric kinase receptors, leading to pSmad1/5/9-mediated induction of BMP target genes. During the blastula and early gastrula stages of vertebrate development, BMP expression peaks ventrally, while expression of the BMP antagonist Chordin is maximal dorsally. Loss of BMP signaling produces dorsalized embryos, while gain of function leads to ventralized phenotypes in a dose-dependent manner, highlighting that tight regulation of the BMP pathway is necessary (reviewed by Rogers and Müller, 2019).

Following bisection, the lateral halves of a *Xenopus* blastula close the wound such that the original dorsal and ventral signaling centers become juxtaposed, allowing the halved embryos to give rise to two properly patterned smaller tadpoles (Fig. 3A) (Moriyama and De Robertis, 2018). Both centers shift by 90°, eventually ending up on opposing sides of the embryo, as shown by pSmad1/5/9 and Chordin staining (Moriyama and De Robertis, 2018). Another BMP

Development (2019) 146, dev177709. doi:10.1242/dev.177709

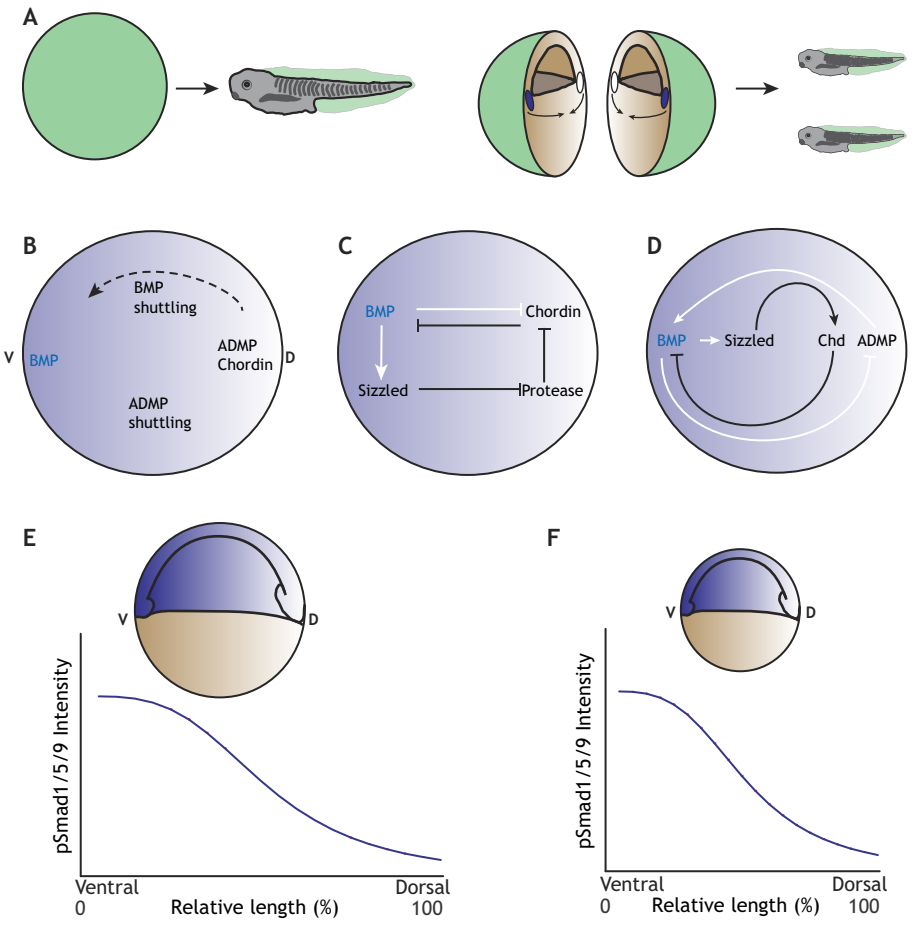

Fig. 3. Scaling of dorsal-ventral patterning. (A) Two properly patterned smaller tadpoles can develop from halved frog embryos (based on De Robertis, 2006; Reversade and De Robertis, 2005). Blue ovals in the halved embryos designate the ventral signaling centers, while white ovals represent the dorsal organizers. Small arrows indicate the direction of wound closure. (B) The expansion-repression model suggests that ADMP and BMP are shuttled ventrally by Chordin, thereby creating a gradient of BMP signaling (blue) (modified, with permission, from Ben-Zvi et al., 2011b). (C) In the long-range accumulation and feedback model, Sizzled stabilizes Chordin levels, thereby limiting its own expression. Through this interaction, size-invariant gradients of BMP activity (blue) and Chordin are established (based on Inomata et al., 2013). (D) In the case of the double-expander model, both Sizzled and ADMP regulate signaling levels by inductive or repressive interactions (based on Ben-Zvi et al., 2014). White arrows in B-D indicate transcriptional interactions, whereas black arrows indicate interactions at the protein level. (E,F) Plot of BMP activity gradients in normal (E) and surgically size-reduced (F) zebrafish embryos, based on the corresponding readout from pSmad1/5/9 antibody staining. The gradient scales relative to embryo length, but the mechanism underlying this scaling is currently unclear (based on Huang and Umulis, 2019).

ligand, ADMP (anti-dorsalizing morphogenetic protein), is expressed at low levels and represses its own expression via positive feedback on BMP, thereby establishing a self-regulatory system (Reversade and De Robertis, 2005). ADMP is indispensable in this system, as the combination of BMP and ADMP determines the shape of the BMP activity gradient (Ben-Zvi et al., 2011b; Reversade and De Robertis, 2005). Facilitated diffusion of BMP and ADMP upon binding to Chordin has been suggested to effectively 'shuttle' BMP activity towards the ventral side away from the Chordin source, which would allow this system to adapt to different embryo sizes (Fig. 3B) (Ben-Zvi et al., 2008). It has therefore been suggested that this network comprises an expansion-repression system (discussed above) for scale-invariant patterning, in which ADMP functions as the expander that is repressed by BMP.

As an alternative, a long-range accumulation and feedback model has recently been suggested (Fig. 3C) (Inomata et al., 2013). This model is based on data showing that the highly diffusible BMP target Sizzled stabilizes Chordin levels by inhibiting its protease-mediated degradation. This in turn feeds back on BMP activity and thus on *sizzled* expression, thereby forming an embryo-wide feedback loop that provides size invariance (Inomata, 2017; Inomata et al., 2013). It is likely that both Sizzled and ADMP act as expanders, and it is possible that they together control robust scaling of DV patterning during *Xenopus* development through a 'double-expander' mechanism (Fig. 3D) (Ben-Zvi et al., 2014).

Immunostaining for pSmad1/5/9 has revealed that a scaled gradient of BMP signaling also accounts for the size invariance of surgically modified zebrafish embryos (Fig. 3E,F) (Huang and Umulis, 2019). A shuttling mechanism in zebrafish, as proposed for *Xenopus*, would require that: (1) the diffusivity of BMP is much smaller than that of Chordin; (2) Chordin enhances BMP diffusion; (3) the half-life of BMP is larger than that of Chordin; and (4) the ventral pSmad1/5/9 peak decreases in the absence of Chordin. However, all of these conditions have been refuted experimentally (Pomreinke et al., 2017; Zinski et al., 2017). The mechanism underlying zebrafish scale-invariant DV patterning is therefore currently unclear, but it is possible that it is regulated by the concentration of one of the BMP signaling inhibitors that might act as a scaling modulator.

Scaling of germ layer patterning

During gastrulation, the inner-to-outer body organization is determined and embryos specify the correct proportions of cells that contribute to the three germ layers: endoderm, mesoderm and ectoderm (Fig. 4A). These decisions are regulated by an activator-inhibitor system comprising Nodal signaling molecules, which induce mesendodermal cell fates, and Lefty proteins, which antagonize Nodal proteins and thus promote ectodermal fates (reviewed by Rogers and Müller, 2019; Schier, 2009). Computational screening and *in vivo* experiments have revealed that the concentration of the highly diffusive Nodal inhibitor Lefty acts as a size sensor (Fig. 4B): after removal of 30% of the cells from the embryonic animal pole (Box 1), the short-range Nodal gradient remains largely unaffected, whereas the highly diffusive inhibitor Lefty is reflected from the new boundary and fills up the smaller patterning field (Almuedo-Castillo et al., 2018). Thus, the domain of Nodal signaling and hence mesendodermal target gene expression shrinks to re-establish the correct germ layer proportions. As differential diffusivity of activators and inhibitors is essential for patterning in this system (Müller et al.,

Development (2019) 146, dev177709. doi:10.1242/dev.177709

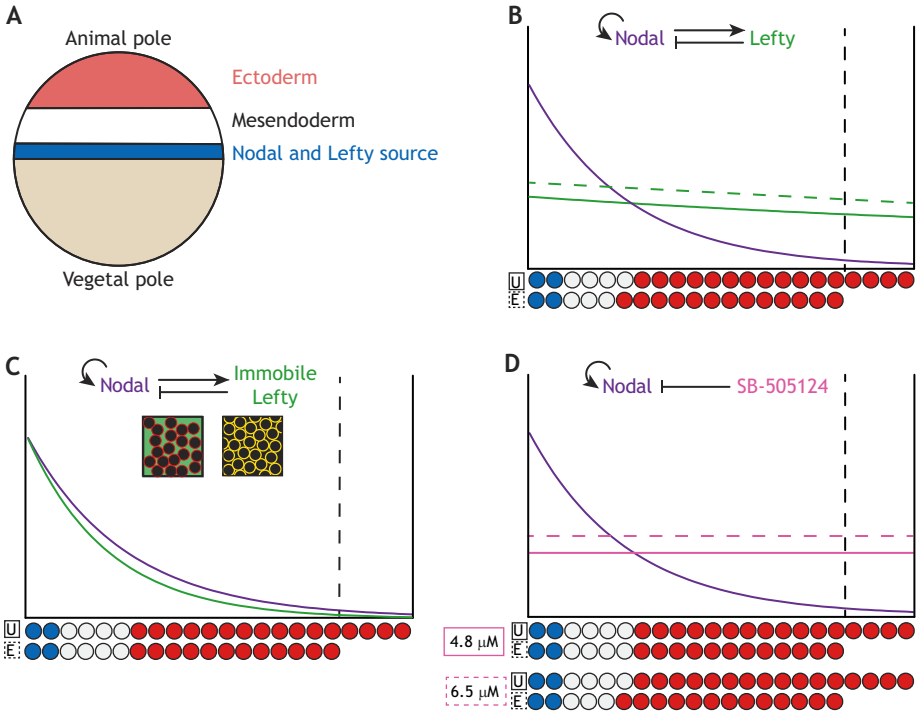

Fig. 4. Scaling of germ layer formation. (A) Schematic of germ layer progenitors in a zebrafish blastula. The marginal cells (blue) are the source of both Nodal and Lefty molecules. Prospective mesendoderm (white) requires high amounts of Nodal signaling, whereas ectoderm progenitors (red) are formed in the absence of Nodal activity. (B) In smaller extirpated embryos, Lefty levels (green) rise and modulate Nodal activity (purple) to scale germ layer proportions. Dashed lines mark the embryo border (black) and Lefty levels in extirpated embryos. Rows of cells below the gradient model symbolize the germ layers in untreated (U) and extirpated (E) embryos. (C) Scaling depends on high Lefty diffusivity. If a membrane-tethered, GFP-binding nanobody (Harmansa et al., 2015) is injected, Lefty-GFP protein binds to the cell membrane (right inset; yellow membranes symbolize the overlay of Lefty-GFP and red cell membranes) instead of being the intercellular space (left inset). Lefty therefore accumulates at the margin and can no longer sense field size for germ layer scaling. (D) *lefty* mutants can be rescued by application of the small-molecule Nodal inhibitor SB-505124, but extirpated (E) embryos require higher levels than untreated ones. All panels are modified, with permission, from Almuedo-Castillo et al. (2018).

2012), embryos do not scale if Lefty diffusion is inhibited (e.g. by tethering Lefty to membranes; Fig. 4C) (Almuedo-Castillo et al., 2018). Strikingly, *lefty* mutants can be rescued by exposure to ectopic small-molecule Nodal inhibitors (Rogers et al., 2017). Surgically shortened *lefty* mutants can also be rescued by inhibitor exposure, but they require higher concentrations than unmanipulated mutants (Fig. 4D) (Almuedo-Castillo et al., 2018), demonstrating that appropriate size-dependent inhibition levels are required to achieve the correct germ layer proportions.

Conceptually, germ layer scaling is achieved through a mechanism involving a size-dependent highly mobile modulator, as introduced earlier. As *lefty* expression is under the control of Nodal signaling (reviewed by Rogers and Müller, 2019), this system can superficially be interpreted as an active modulator or induction-contraction network (Nesterenko and Zaraisky, 2019). However, Lefty-mediated size control in zebrafish embryos can also be uncoupled from Nodal signaling by creating artificial Lefty sources that are not part of a feedback mechanism (Almuedo-Castillo et al., 2018), showing that a passive modulator system is sufficient to explain scale-invariant patterning in this context.

Scaling during neural tube patterning

The vertebrate neural tube is patterned into 13 populations of different neuronal progenitors along the DV axis (Alaynick et al., 2011). This pattern is regulated by two signaling centers: the dorsal roof plate, which secretes BMP and Wnt signals, and the floor plate and notochord, which secrete Sonic hedgehog (Shh) (Fig. 5A, top) (Briscoe et al., 2001; Liem et al., 2000, 1997; Roelink et al., 1995). Thus, the neural tube is patterned by opposing gradients of signaling molecules. However, cells do not seem to measure the ratio between BMP and Shh, as would be the case for an opposing gradient model, as cells that are exposed to high levels of both signals adopt either dorsal or ventral rather than intermediate fates (Collins et al., 2019 preprint; Zagorski et al., 2017).

During development, the progenitor domains in the neural tube undergo changes in size as the tissue grows (Box 2). Unlike other patterning systems, the morphogen gradients do not scale during growth; after the initial cell fate specification phase, cell type-specific differentiation dynamics control domain proportions (Fig. 5A) (Kicheva et al., 2014). This has been elegantly demonstrated in studies of mice that are heterozygous for a deletion in *rpl24*, which encodes a large ribosomal subunit. These mice have about 20% smaller neural tubes, but they exhibit the same tissue proportions as wild-type mice (Fig. 5A, bottom) (Kicheva et al., 2014). How size feeds back on differentiation rate is not precisely understood, but it has been suggested that post-mitotic neurons are involved (Kicheva et al., 2014).

A different mechanism has been found in artificially size-reduced fish embryos. Here, a variant of the expansion-repression model is thought to scale the ventral Shh gradient via the secreted matrix protein Scube2 (Fig. 5B) (Collins et al., 2019 preprint; Shilo and Barkai, 2017). Scube2 displays the classical features of an expander: it is repressed by Shh signaling, and it cell non-autonomously enhances the range of Shh signaling (Collins et al., 2019 preprint). How the dorsal BMP gradient adjusts its size during neural tube patterning is not yet known, but it is tempting to speculate that a similar expansion-repression mechanism might act in this context, as the secreted Chordin stabilizer Sizzled (and potentially *admp* in species that possess this gene, such as zebrafish) enables the early embryonic BMP gradient to scale in an expander-like manner (Ben-Zvi and Barkai, 2010; Ben-Zvi et al., 2014, 2008; Inomata et al., 2013).

Somite formation

During development, somites are formed from the presomitic mesoderm (PSM) in an anterior-to-posterior sequence. This process can be described by a clock-wavefront model (Cooke and Zeeman, 1976; reviewed by Oates et al., 2012). In this model, tissue polarity is controlled by posterior-to-anterior signaling gradients of FGFs and Wnts, and an opposing gradient of retinoic acid (Fig. 6A) (Aulehla and Pourquié, 2010). The frequency of somite formation is controlled by a clock, which consists of a system of coordinated oscillators in PSM cells

Development (2019) 146, dev177709. doi:10.1242/dev.177709

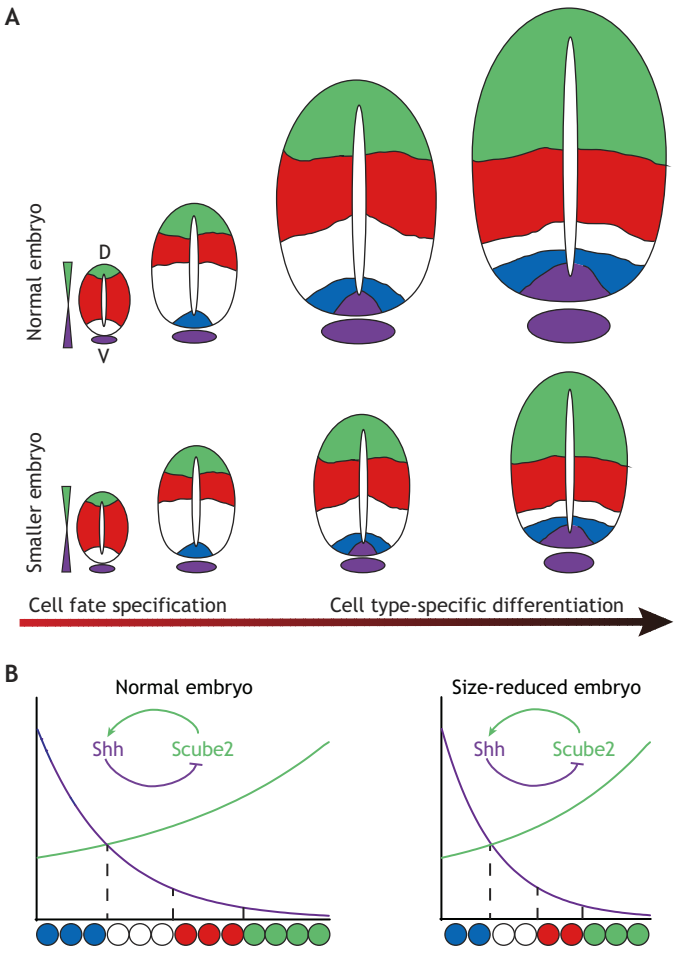

Fig. 5. Scaling of neural tube patterning. (A) Scaling of dorsal-ventral neural tube patterning during growth in mouse and chick. Schematics of sections through normal (top) and mutant (smaller, bottom) neural tubes at different stages. The colors represent different populations of neural progenitors. Putative opposing gradients of Shh (purple) and Wnt/BMP (green) are shown on the left of the neural tube schematics. Cell fate is specified early on, but proportions of tissues are not maintained during growth. Instead, cell type-specific differentiation dynamics pattern the neural tube dorsoventrally. Proportions of neural progenitors are, however, conserved in downscaled mutant neural tubes (modified, with permission, from Kicheva et al., 2014). (B) Neural tube patterning also scales in experimentally size-reduced zebrafish embryos. In this system, an expansion-repression-based feedback mechanism between the ventral Shh gradient and the expander protein Scube2 enables size-invariant patterning (based on Collins et al., 2019 preprint).

that exhibits species-specific timing. For example, in zebrafish a somite is formed every 25 min, in frogs or chicken every 90 min, and in mouse every 2 h (Gomez et al., 2008; Schröter et al., 2008). The position of somite formation is determined by a travelling wavefront that freezes the oscillating cells and thereby causes formation of a new somite. The main oscillator genes are orthologs of the *hairy and enhancer of split* family (*her* or *hes*) as well as components of the Wnt, FGF and Delta/Notch pathways (Oates et al., 2012; Palmeirim et al., 1997).

As mentioned above, the first evidence to suggest that somite size scales with body size was provided by Cooke in 1975 (Cooke, 1975), but the mechanism underlying this scaling remained unclear for a long time. Conceivably, four factors could contribute to the size-invariance of somite patterning: the clock period, the axis elongation speed, the wavelength or the gradients of the wavefront (Ishimatsu et al., 2019, 2018). PSM cells are known to proliferate, but more cells are lost to the forming somites, and over time the PSM shrinks. However, it is not entirely clear whether PSM length and the length of the formed somites are correlated (Cooke, 1975; Gomez et al., 2008; Ishimatsu et al., 2018; Lauschke et al., 2013). Changes in the period of the segmentation clock have been shown to change somite length, but this does not scale with embryo length during normal development (Harima et al., 2013; Herrgen et al., 2010; Schröter and Oates, 2010). Likewise, studies in surgically size-reduced zebrafish embryos have shown that neither the clock period nor the axis elongation speed scale in this case (Ishimatsu et al., 2018).

What, then, does control scaling in this context? The wavelength of the *her1* gene does not scale with normal PSM size reduction during development, but it does in size-decreased embryos (Ishimatsu et al., 2018). In addition, immunohistochemistry for the FGF effector ERK, together with FRET-sensor experiments, have revealed that the FGF gradient scales both during normal development and after surgery (Fig. 6B,C). Thus, a suggested mechanism for this 'clock and scaled gradient' system involves negative feedback of newly formed somites on FGF that leads to gradient shortening. The precise molecular mechanism is not yet clear, but multiple options come to mind. The opposing gradients of Wnt/FGF and somite-derived retinoic acid could constitute an opposing gradient system that allows scaling (Oates et al., 2012). Alternatively, feedback-based mechanisms could control somite size, as Wnt and FGFs have been shown to act in auto-regulatory feedback loops in other systems (e.g. during regeneration, discussed below).

Scaling during regeneration

Varying degrees of regenerative capacity are found in almost all animals. Amphibians have remarkable regenerative abilities that enable them to regrow an entire limb or reconnect a severed spinal cord. Cnidarians (such as Hydra) and planarians (such as *Schmidtea mediterranea*) are even capable of whole-body regeneration (reviewed

Box 2. Scaling during growth

During development, organs and organisms grow to a defined size. Similar to the mechanisms discussed in the main text, scaling during growth can be achieved if the source scales with tissue size (Aguilar-Hidalgo et al., 2018). Opposing gradients can scale to some extent, although not in tissues that increase ∼10-fold in size, such as the Dpp-controlled *Drosophila* imaginal discs (McHale et al., 2006; Romanova-Michaelides et al., 2015). Another model suggests that morphogen degradation decreases with growth by modulator molecule dilution (Wartlick et al., 2011). Feedback-based systems such as the expander-repression model can also scale with growth (Ben-Zvi and Barkai, 2010; Ben-Zvi et al., 2011a,b; Hamaratoglu et al., 2011) but might be too slow for the cell cycles in *Drosophila* (Romanova-Michaelides et al., 2015). Conversely, the advection-dilution model, which suggests that morphogens travel away from the source along with cells, can account for fast growth but requires higher morphogen mobility than was measured (Averbukh et al., 2014; Wartlick et al., 2011). Finally, theoretical data show that advection alone can, in principle, also achieve perfect scaling (Fried and Iber, 2014). It is conceivable that a combination of these mechanisms controls scaling during growth.

In addition to scaling of the morphogen gradient, a mechanism for growth control is required. It has been suggested that mechanical forces caused by growth and migration support the readout of absolute morphogen levels in achieving growth control (Aegerter-Wilmsen et al., 2007; Hufnagel et al., 2007). Alternatively, cells could read out relative instead of absolute gradient levels in space and time, and decide when to stop proliferating (Day and Lawrence, 2000; Rogulja and Irvine, 2005; Wartlick et al., 2011). However, in *Drosophila* the Dpp gradient appears to be dispensable for later wing disc development, suggesting a Dpp-independent mechanism for growth termination (Akiyama and Gibson, 2015).

Development (2019) 146, dev177709. doi:10.1242/dev.177709

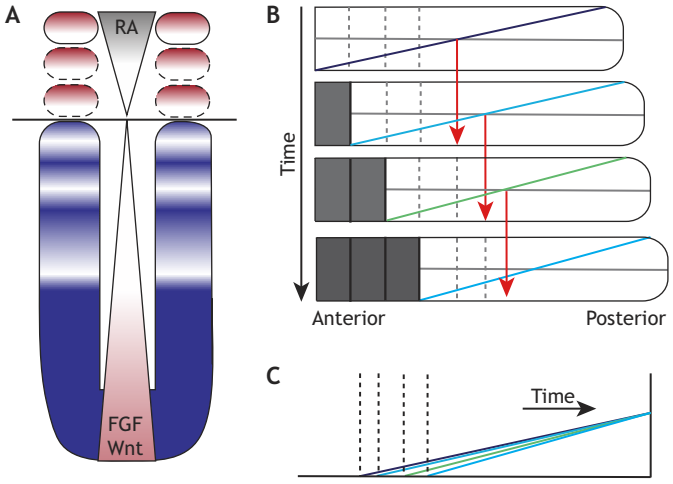

Fig. 6. Scaling of somite formation. (A) Schematic of the vertebrate segmentation clock (based on Oates et al., 2012). In the presomitic mesoderm, oscillatory gene expression (blue and white) is arrested at the wavefront formed by opposing Wnt/FGF and retinoic acid (RA) gradients. Freshly arrested segments (dashed lines) later form somites. (B) Scaling through the 'clock and scaled gradient' model. As in the classical clock-wavefront model, arrested segments form somites with a delay, and cells are arrested when levels of the FGF gradient (linear gradients in shades of blue and turquoise) fall below a threshold (gray horizontal line). Additionally, the FGF gradient is modulated by the somites and therefore scales with the length of the presomitic mesoderm. (C) Over time, the gradient becomes steeper and the somites shorter, as seen using superimposition of the gradients at different time points shown in B. The same mechanism can also account for somite scaling in surgically manipulated embryos (modified, with permission, from Ishimatsu et al., 2018).

by Ivankovic et al., 2019; Joven et al., 2019; Vogg et al., 2019b). During regeneration, animals recapitulate various embryonic processes and developmental pathways, indicating that scaling of positional information is also necessary. Importantly, regenerating tissues must grow to the size of an adult animal. This process appears even more complex than embryonic size invariance, as signaling must first scale to accommodate the reduced body size and, subsequently, rescaling during growth must be accomplished (Box 2). Additionally, regeneration does not have a fixed starting point but is initiated at a random point of wounding, suggesting the need for a self-organizing system (Stückemann et al., 2017). In this section, we discuss mechanisms of size control in Hydra (Vogg et al., 2019a), planarians (Stückemann et al., 2017; Werner et al., 2015) and amphibians (Bryant et al., 2017; Vincent et al., 2015) from the perspective of positional information.

Hydra

The freshwater polyp Hydra is capable of remarkably size-invariant regeneration. As Lewis Wolpert stated in his 1969 publication: 'a fragment of hydra, one-hundredth its volume can give rise to an almost complete animal' (Wolpert, 1969). The Hydra body consists of an apical head structure with tentacles and a dome surrounding the mouth, called a hypostome, a body column and a basal foot structure (Fig. 7A). Transplantation experiments conducted more than 100 years ago revealed that the hypostome has inducing capacity similar to what was later termed an embryonic organizer (Browne, 1909). Adult Hydra polyps retain a permanent stem cell population, and axial polarity is maintained by signals from the hypostome (Hobmayer et al., 2000). If the head and foot parts of the animal are removed, the gastric section regenerates and maintains the original polarity (Wilby and Webster, 1970). After mid-gastric bisection, both pieces regenerate the missing body parts, with head-organizer activity being established after 3 h in the head-regenerating tip and retained for about 2 days (MacWilliams, 1983).

An RD system has been proposed to explain the inductive abilities of the head organizer and the transplantation and regeneration data (Gierer and Meinhardt, 1972). In this model, the head region contains high levels of an activator that, together with its long-range inhibitor, is thought to form a gradient across the body axis. In a system like this, any part of the gastric region will retain its polarity even if the gradient is shallow (Gierer and Meinhardt, 1972).

A number of molecules that might be involved in this activator-inhibitor system have been identified. The role of the activator, a promoter of head identity, is provided by Wnt signaling (Hobmayer et al., 2000), and the transcription factor HySp5 has recently been identified as the inhibitor of the system (Vogg et al., 2019a). HySp5 is a target gene of Wnt signaling but, in contrast to the predictions of the RD theory, it acts cell-autonomously and is not diffusible (Vogg et al., 2019a). It has been shown, however, that multi-component RD systems can also comprise non-diffusible locally acting elements (Marcon et al., 2016). HySp5 could therefore act as a spatially fixed capacitor that might integrate other diffusible signals (Landge et al., 2019; Marcon et al., 2016).

Owing to their original axial polarity, head and foot regeneration differ to some extent. After mid-body section, the formation of a new organizer in the head-regenerating tip is likely triggered by elevated Wnt levels in direct response to wounding via apoptosis (Chera et al., 2009; Galliot, 2013). After this initial Wnt burst, from day 2 onwards, these signals re-establish the gradient along the body axis (Gufler et al., 2018; MacWilliams, 1983). Models indicate that, by removing the area of high activator (i.e. the head part), the remaining inhibitor decays and a new maximum can arise due to fluctuations in the source cells – in this case the apoptotic Wnt burst – or by retaining the original polarity based on relative activator levels (Fig. 7A) (Gierer and Meinhardt, 1972; Meinhardt, 2009).

Regeneration of the Hydra foot, by contrast, is thought to resemble a wound healing response (Galliot, 2013). Therefore, foot regeneration does not require additional positional information: a new foot structure can be generated wherever the activator-to-inhibitor ratio is lowest. This gradient scales to the new body size, because the remaining inhibitor has a smaller field in which to disperse and thus the activation is reduced (Fig. 7A) (Meinhardt, 2009). Thus, this system displays properties consistent with the modulator models discussed earlier.

Planaria

Many planarians, such as *Schmidtea mediterranea* or *Planaria maculata*, can regenerate full animals after being cut into pieces, and even one 279th of a dissected planarian flatworm can give rise to a normally patterned individual over time (Morgan, 1898). The workhorse of planarian regeneration is a population of embryonic-like stem cells termed neoblasts that are found throughout the adult body (reviewed by Reddien, 2018). Positional information during homeostasis is maintained by muscle cells (Witchley et al., 2013). After transversal mid-body bisection, the first challenge is to re-establish proper anterior-posterior polarity. An activator-inhibitor Turing-like RD system has been suggested to pattern the animal during development and regeneration (Werner et al., 2015), but Turing models in their simplest form do not scale and create repeated patterns (Müller and Nüsslein-Volhard, 2016; Murray, 2013). If this was the patterning mechanism, a flatworm could end up with two heads or tails (Fig. 7B) (Cooke, 1975; Werner et al., 2015). However, if an additional molecule – an expander – is introduced, the system can spontaneously self-organize and also scale

Development (2019) 146, dev177709. doi:10.1242/dev.177709

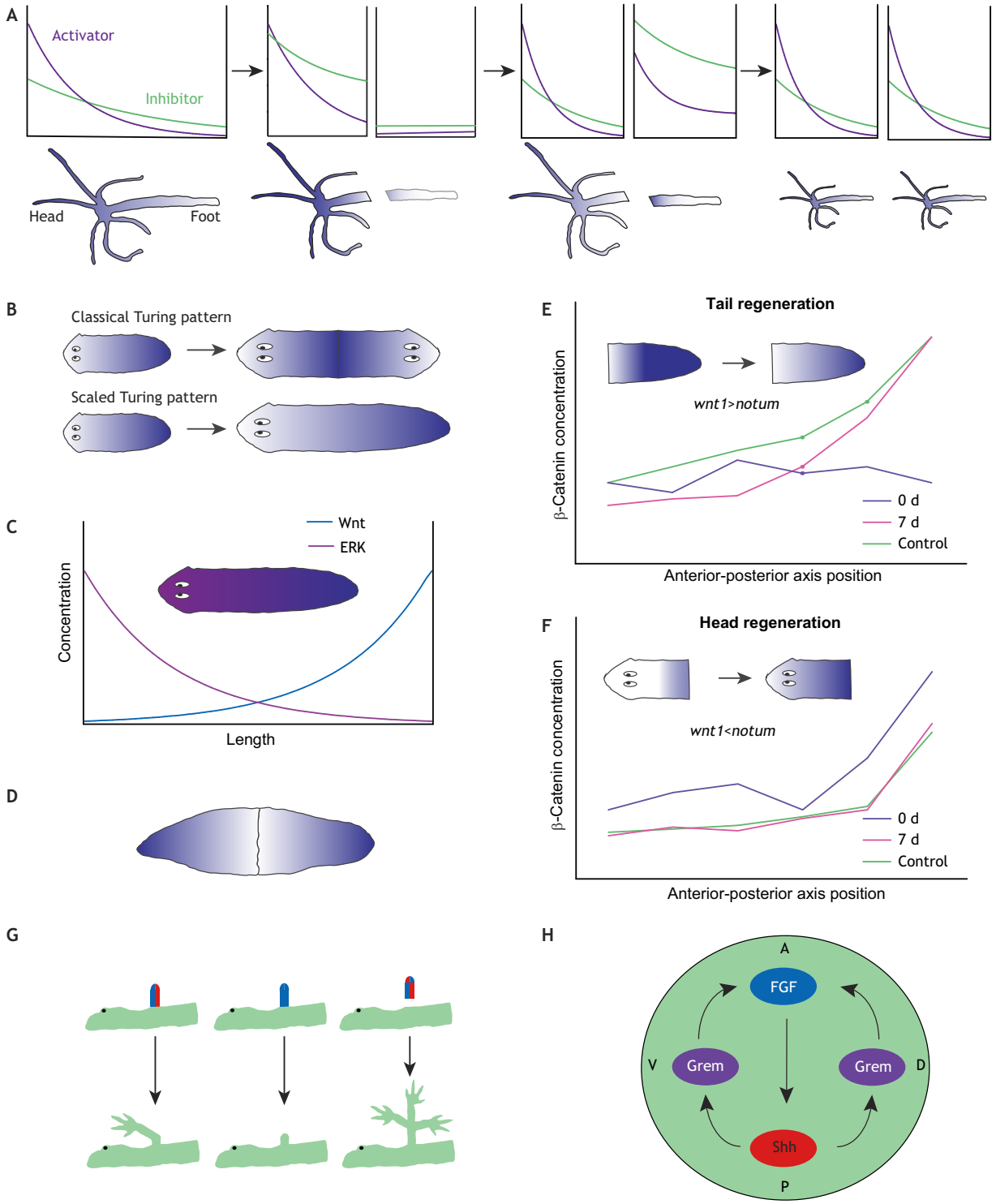

Fig. 7. Scaling during regeneration. (A) Re-establishment of polarity in regenerating Hydra head and foot parts after mid-gastric bisection. In the head segment, polarity is retained and the proper scale of activator and inhibitor is regained by rising concentrations of the inhibitor. In the regenerating foot part, polarity is likely lost and, after decay of the remaining inhibitor, new polarity can arise by amplifying fluctuations, like the Wnt burst induced after wounding (based on Meinhardt, 2009). (B) Planarians also retain polarity during regeneration. They cannot rely on a simple Turing system, as this would form repeated patterns, so they also need a size-invariant ('scaled') patterning system (based on Werner et al., 2015). (C) A potential scaling mechanism involves opposing gradients of β-catenin and ERK signaling. (D) However, a Wnt gradient can also exist in the absence of an anterior antagonist, as shown by double-tailed planarians with an intact Wnt gradient. (E,F) The posterior-to-anterior Wnt gradient is entirely re-established 7 days after injury in head and tail regenerating embryos alike. Head versus tail regeneration is thought to be controlled by a *wnt1*/*notum* switch (C-F; redrawn, with permission, from Stückemann et al., 2017). (G) Axolotls can also regenerate their limbs if anterior (blue) and posterior (red) parts of the limb are present. If tissue of the same positional information is grafted in lieu of the opposing one, no regeneration takes place. If multiple borders of opposing polarity are created by grafting a piece of tissue inversely onto the wound site, multiple limbs are regenerated. (H) The underlying genetic mechanism consists of a Shh/Grem/FGF network. It is currently unknown how size invariance is achieved, but this is likely due to scaling of the signaling gradients (G,H; based on Tanaka, 2016).

Development (2019) 146, dev177709. doi:10.1242/dev.177709

(Werner et al., 2015). In this system, the expander must negatively regulate both the activator and the inhibitor, and it must be degraded by the inhibitor. Another explanation for the re-establishment of anterior-posterior polarity in planarian regeneration, supported by the shape of signaling gradients in double-tailed individuals, is that two signaling centers exist at opposing poles, thus forming part of a 'dual gradients' model (Fig. 7C,D) (Stückemann et al., 2017).

Like the head organizer of Hydra, the planarian posterior signaling center comprises a Wnt feedback loop; accordingly, Wnt inhibition forces head formation and inhibits tail regeneration (Gurley et al., 2008; Iglesias et al., 2008; Petersen and Reddien, 2008). Consequently, the levels of Wnt signaling increase or decrease at the wound sites of tail or head regenerating pieces, respectively, within the first 24 h and return to their normal levels within 7 days (Fig. 7E,F) (Gurley et al., 2010; Petersen and Reddien, 2009; Stückemann et al., 2017). This is thought to be caused by a generic wound response mediated by a *wnt1/notum* switch that represses Wnt-dependent tail regeneration in anterior-facing wounds (Fig. 7E,F) (Gurley et al., 2010; Petersen and Reddien, 2009, 2011; Stückemann et al., 2017; Wenemoser et al., 2012; Wurtzel et al., 2015). In agreement with both the expander (Werner et al., 2015) and the dual gradients model (Stückemann et al., 2017), uniformly high levels of β-catenin cause uniform expression of tail genes. Knockdown of the Wnt pathway, however, induces the formation of additional heads along the body axis that are properly patterned, supporting the dual gradient model (Iglesias et al., 2008; Stückemann et al., 2017).

If the dual gradients model holds true, what might be the nature of the signal that opposes the Wnt gradient? Studies have shown that a gradient of ERK signaling that is maximal anteriorly (Fig. 7C) could fulfill the role as the opposing gradient to the posterior-to-anterior Wnt gradient (Agata et al., 2014; Tasaki et al., 2011; Umesono et al., 2013). Likewise, Hh signaling has a regulating effect on Wnt signaling, thereby contributing to polarity (Rink et al., 2009; Yazawa et al., 2009).

Although a system of opposing gradients would be able to scale by itself, computational analyses have suggested that the active transport of morphogens can aid scaling (Pietak et al., 2019). In this model, Hedgehog molecules are transported along axons by kinesin in an anterior-to-posterior direction, and a notum-inducing factor is subject to dynein transport in the other direction. In this way, morphogen gradients form relative to the direction of the neuronal vector field independent of tissue size and symmetry (Pietak et al., 2019). Thus, three different models are currently able to explain polarity re-establishment in regenerating planarians, and more work is required to unify these theoretical frameworks.

Amphibians

Regeneration in salamanders is initiated after wound closure by the accumulation and proliferation of diverse mesenchymal cells that form the blastema: a region of undifferentiated cells that is crucial for regeneration. Proliferation and subsequent differentiation of these cells into tail elements (myotomes) or limb elements then proceeds until the right amount of limb or tail is regrown. After distal limb amputation, a hand is regenerated, while a more-proximal injury leads to the formation of a whole arm. However, blastema cells from the hand are not able to regenerate a whole arm when transplanted into a more proximal position, suggesting that the original positional information of the tissue is retained during regeneration (Pescitelli and Stocum, 1980; Roensch et al., 2013). Interestingly, the duration of the regeneration phase is independent of the size of the structure. In the first phase of tail regeneration (15 days after amputation), for example, blastema cells are in a maximum growth phase, independent of their proximal-distal position. However, proximal cells differentiate at a lower rate while blastema cells continue proliferating. This surplus of stem cells is thought to cause the faster growth observed after proximal injuries compared with distal injuries (Bryant and Gardiner, 2016; Vincent et al., 2015). Therefore, the amount of tissue that is regenerated appears to be controlled by cell-cycle gradients that in turn are thought to be regulated by morphogen gradients (Bryant and Gardiner, 2016).

Strikingly, regeneration does not occur if tissues of the same polarity are in contact. If, for example, an anterior part is grafted to replace the posterior part and thus a double anterior limb is created, regeneration cannot proceed. On the contrary, supernumerary limbs are produced if the polarity is surgically inverted, such that multiple juxtapositions of anterior and posterior tissues occur (Fig. 7G) (Butler, 1955; Iten and Bryant, 1975). This suggests that whenever anterior blastema cells are positioned next to posterior ones, a signaling center that promotes growth is formed (Tanaka, 2016).

The molecular network underlying this phenomenon consists of anterior FGF8, posterior Shh and the BMP inhibitor Gremlin (Grem) (Fig. 7H) (Nacu et al., 2016). Additional proximal-distal positional information is provided by a retinoic acid gradient (McCusker et al., 2014), with connective tissue being the primary responsive cell type (Kragl et al., 2009; Nacu et al., 2013). The FGF-Shh system is reminiscent of that observed during embryonic limb development, where growth is maintained by FGF8 signaling from apical tissue, which in turn requires Shh signaling from the posterior zone of polarizing activity (ZPA) in order to be maintained (Chiang et al., 2001) (for a review of vertebrate limb development, see Saxena et al., 2016). In this system, Grem functions as a relay between Shh and FGF signaling, and growth terminates once a population of cells unable to express *grem* is established (Scherz et al., 2004). But how, if at all, does this system scale? Whereas during embryogenesis the tissue is patterned while it grows, the field size during regeneration is that of an adult limb. It is therefore likely that the FGF, Grem and Shh gradients do scale in this context, although this has not yet been experimentally demonstrated (Tanaka, 2018). A version of the expander mechanism for scaling would be attractive: in this scenario, mesenchymal BMP signaling inhibits FGF signaling from the anterior mesenchyme, and BMP in turn is inhibited by Grem, which depends on Shh signaling from the ZPA. This relay could be used to measure the distance between the anterior mesenchyme and the ZPA and thus field size. It should also be noted that the limb patterning network in axolotls is based on FGF, Shh and RA, but also on canonical Wnt signaling, as regeneration does not occur if Wnt signaling is inhibited (Kawakami et al., 2006). Therefore, it is tempting to speculate that this might be homologous to the first position-independent phase of *wnt* expression in Hydra regeneration (Gufler et al., 2018) and the generic wound response in planarians (Wenemoser et al., 2012; Wurtzel et al., 2015).

Overall, these studies indicate that a number of molecular pathways could together provide scaling, but more data are required before speculations about their mechanisms of action can be converted into useful hypotheses. For example, visualization of the signaling molecules involved is needed to clarify whether these form gradients and whether those gradients scale. Additionally, knockdown and uniform rescue experiments could provide information as to whether gradients are required for regeneration.

Conclusions and perspectives

Over the past 50 years, Lewis Wolpert's concept of positional information (Wolpert, 1968, 1969) has been fundamental for the

Development (2019) 146, dev177709. doi:10.1242/dev.177709

Box 3. Scaling in evolution

Species can vary considerably in size, yet their morphological proportions often remain unchanged. How does this size-invariance come about? In different fly species, gap gene patterns and the shape of the underlying Bicoid gradient scale over size differences of about fivefold, although diffusion itself appears to be unchanged between species (Gregor et al., 2005, 2008). In the closely related fish species *Danio rerio* and *Devario aequipinnatus*, on the other hand, there seems to be no interspecies scaling, as they display differently shaped gradients of BMP (Huang and Umulis, 2019). In this case, however, target gene expression data is missing and only the gradient of one molecule within a complex network is known. This leaves room for future discoveries regarding interspecies scaling mechanisms. A novel mechanism of interspecies scaling has been discovered in the avian neural tube, where the cell-autonomous response to a Shh signaling gradient is altered but not the gradient itself (Uygur et al., 2016). Fixing cell fate specification to a developmental time point where embryos of different species have similar size, supplemented by a later growth and proliferation phase, also allows for scaling of morphological proportions without needing to change gradient shape (Kicheva et al., 2014). Selection experiments in *Drosophila* have revealed shape-adjustment of the Bicoid gradient in response to breeding for size extremes (Cheung et al., 2011). Along these lines, the amount of *bicoid* mRNA deposited in the localized source at the anterior pole scales with embryo size, consistent with a boundary-driven scaling mechanism. Interestingly, in another breeding experiment, near-perfect scaling of the Bicoid range was observed, but the mechanism is currently unclear (Cheung et al., 2014). Finally, mice selected for longer tibiae over several generations display mutations in the enhancers of effector genes of bone morphogenesis (Castro et al., 2019), also suggesting scaling by response of the target tissue.

field of developmental biology. A major motivation for Wolpert's positional information concept was the need for a mechanism to explain how differently sized embryos scale their tissue proportions. The simple gradients that Wolpert proposed have subsequently inspired new theories, and recent experimental and theoretical advances over the last 15 years have allowed direct tests of these ideas.

Four major models have been proposed that can account for scale-invariant patterning: (1) scaling by specific boundary conditions; (2) modulating signaling gradients by highly diffusible molecules; (3) using opposing gradients; and (4) feedback-based systems. There is no reason to believe that only one of these models is applicable to every case. On the contrary, it appears that even the same signaling pathways can scale using different strategies. Shh, for example, is size adjusted in the zebrafish neural tube via a feedback mechanism, while its size invariance in avian interspecies scaling (Box 3) is based on differential target tissue responsiveness. With more experimental data from different systems, our understanding of the general mechanisms of scaling will expand.

Currently many scaling scenarios are only partially understood. The BMP gradient in zebrafish DV patterning, for example, has been shown to scale, but the underlying mechanism is unclear. A shuttling function, as suggested for *Xenopus*, has been ruled out. It is tempting to speculate that BMP signaling scales analogously to the Nodal pathway, with Sizzled playing the role of Lefty, because Sizzled is diffusible, negatively feeds back on BMP, and is a strong target of BMP signaling, just like Lefty for Nodal (Dubrulle et al., 2015). Interestingly, *Xenopus* BMP signaling and zebrafish Nodal signaling appear to use rather different mechanisms for scale-invariant patterning, although both ligands belong to the TGFβ superfamily and thus likely have similar properties. Therefore, analyses of amphibian germ layer and fish DV patterning hold the potential to greatly advance our understanding of scaling and patterning mechanisms in general.

The similarities and parallels between development and regeneration are striking. Molecules that are used for the initial patterning during development are also re-deployed during regeneration. The Wnt pathway, for example, is crucial for determining anterior-posterior polarity in both development and regeneration, and in the case of planarians and cnidarians also in maintaining this polarity once a steady state is reached. Furthermore, there are strong resemblances mechanistically, such that the dilution of inhibitors or expanders in both contexts can act to scale tissue proportions.

Moving forward, it will be interesting to see many of the gaps in our knowledge close and new approaches emerge. For example, most studies have focused on artificially reducing the size of embryos, but it would also be illuminating to increase embryo size in order to determine the limits of scaling. Intra-species experiments also have the potential to not only broaden our understanding of development, but also aid our understanding of evolution. Finally, *ex vivo* systems or stem cell-based organoids hold enormous potential, as illustrated by their application to study somite development and eye cup formation, where organoids from mice and human recapitulate the species-specific size and timing differences (Ader and Tanaka, 2014; Diaz-Cuadros et al., 2019 preprint; Matsuda et al., 2019 preprint; Nakajima et al., 2018).

Acknowledgements

We are grateful to Katherine W. Rogers and Alexandra Schauer for helpful discussions.

Competing interests

The authors declare no competing or financial interests.

Funding

The authors' research is supported by the Max-Planck-Gesellschaft and a European Research Council Starting Grant (*QUANTPATTERN*).

References

Ader, M. and Tanaka, E. M. (2014). Modeling human development in 3D culture. *Curr. Opin. Cell Biol.* **31**, 23-28. doi:10.1016/j.ceb.2014.06.013

Aegerter-Wilmsen, T., Aegerter, C. M., Hafen, E. and Basler, K. (2007). Model for the regulation of size in the wing imaginal disc of Drosophila. *Mech. Dev.* **124**, 318-326. doi:10.1016/j.mod.2006.12.005

Agata, K., Tasaki, J., Nakajima, E. and Umesono, Y. (2014). Recent identification of an ERK signal gradient governing planarian regeneration. *Zoology (Jena)* **117**, 161-162. doi:10.1016/j.zool.2014.04.001

Aguilar-Hidalgo, D., Werner, S., Wartlick, O., González-Gaitán, M., Friedrich, B. M. and Jülicher, F. (2018). Critical point in self-organized tissue growth. *Phys. Rev. Lett.* **120**, 198102. doi:10.1103/PhysRevLett.120.198102

Akiyama, T. and Gibson, M. C. (2015). Decapentaplegic and growth control in the developing Drosophila wing. *Nature* **527**, 375-378. doi:10.1038/nature15730

Alaynick, W. A., Jessell, T. M. and Pfaff, S. L. (2011). SnapShot: spinal cord development. *Cell* **146**, 178-178.e1. doi:10.1016/j.cell.2011.06.038

Almuedo-Castillo, M., Bläßle, A., Mörsdorf, D., Marcon, L., Soh, G. H., Rogers, K. W., Schier, A. F. and Müller, P. (2018). Scale-invariant patterning by size-dependent inhibition of Nodal signalling. *Nat. Cell Biol.* **20**, 1032-1042. doi:10.1038/s41556-018-0155-7

Aulehla, A. and Pourquié, O. (2010). Signaling gradients during paraxial mesoderm development. *Cold Spring Harb. Perspect. Biol.* **2**, a000869. doi:10.1101/cshperspect.a000869

Averbukh, I., Ben-Zvi, D., Mishra, S. and Barkai, N. (2014). Scaling morphogen gradients during tissue growth by a cell division rule. *Development* **141**, 2150-2156. doi:10.1242/dev.107011

Ben-Zvi, D. and Barkai, N. (2010). Scaling of morphogen gradients by an expansion-repression integral feedback control. *Proc. Natl. Acad. Sci. USA* **107**, 6924-6929. doi:10.1073/pnas.0912734107

Ben-Zvi, D., Shilo, B. Z., Fainsod, A. and Barkai, N. (2008). Scaling of the BMP activation gradient in Xenopus embryos. *Nature* **453**, 1205-1211. doi:10.1038/nature07059

Ben-Zvi, D., Pyrowolakis, G., Barkai, N. and Shilo, B. Z. (2011a). Expansion-repression mechanism for scaling the Dpp activation gradient in Drosophila wing imaginal discs. *Curr. Biol.* **21**, 1391-1396. doi:10.1016/j.cub.2011.07.015

Ben-Zvi, D., Shilo, B. Z. and Barkai, N. (2011b). Scaling of morphogen gradients. *Curr. Opin. Genet. Dev.* **21**, 704-710. doi:10.1016/j.gde.2011.07.011

Ben-Zvi, D., Fainsod, A., Shilo, B. Z. and Barkai, N. (2014). Scaling of dorsal-ventral patterning in the Xenopus laevis embryo. *BioEssays* **36**, 151-156. doi:10.1002/bies.201300136
Bollenbach, T., Kruse, K., Pantazis, P., González-Gaitán, M. and Jülicher, F. (2007). Morphogen transport in epithelia. *Phys. Rev. E Stat. Nonlin. Soft Matter Phys.* **75**, 011901. doi:10.1103/PhysRevE.75.011901
Boveri, T. (1901). Über die Polarität des Seeigeleies. *Verhandl. Phys.Med. Ges. Würzburg* **34**, 145-176.
Briscoe, J., Chen, Y., Jessell, T. M. and Struhl, G. (2001). A hedgehog-insensitive form of patched provides evidence for direct long-range morphogen activity of sonic hedgehog in the neural tube. *Mol. Cell* **7**, 1279-1291. doi:10.1016/S1097-2765(01)00271-4
Browne, E. N. (1909). The production of new hydranths in Hydra by the insertion of small grafts. *J. Exp. Zool.* **7**, 1-23. doi:10.1002/jez.1400070102
Bruns, E. (1931). Experimente über das Regulationsvermögen der Blastula von Triton taeniatus und Bombinator pachypus. *Roux Arch. Entwicklungsmech.* **123**, 682-718. doi:10.1007/BF01380650
Bryant, S. V. and Gardiner, D. M. (2016). The relationship between growth and pattern formation. *Regeneration (Oxf)* **3**, 103-122. doi:10.1002/reg2.55
Bryant, D. M., Sousounis, K., Farkas, J. E., Bryant, S., Thao, N., Guzikowski, A. R., Monaghan, J. R., Levin, M. and Whited, J. L. (2017). Repeated removal of developing limb buds permanently reduces appendage size in the highly-regenerative axolotl. *Dev. Biol.* **424**, 1-9. doi:10.1016/j.ydbio.2017.02.013
Butler, E. G. (1955). Regeneration of the urodele forelimb after reversal of its proximo-distal axis. *J. Morphol.* **96**, 265-281. doi:10.1002/jmor.1050960204
Castro, J. P. L., Yancoskie, M. N., Marchini, M., Belohlavy, S., Hiramatsu, L., Kučka, M., Beluch, W. H., Naumann, R., Skuplik, I., Cobb, J., et al. (2019). An integrative genomic analysis of the Longshanks selection experiment for longer limbs in mice. *eLife* **8**, e42014. doi:10.7554/eLife.42014
Chabry, L. (1887). L'embryologie normale & tératologique des Ascidies simples. *J. Anat. Physiol. Norm. Pathol. Homme Anim.* **23**, 167-319.
Chera, S., Ghila, L., Dobretz, K., Wenger, Y., Bauer, C., Buzgariu, W., Martinou, J. C. and Galliot, B. (2009). Apoptotic cells provide an unexpected source of Wnt3 signaling to drive hydra head regeneration. *Dev. Cell* **17**, 279-289. doi:10.1016/j.devcel.2009.07.014
Cheung, D., Miles, C., Kreitman, M. and Ma, J. (2011). Scaling of the Bicoid morphogen gradient by a volume-dependent production rate. *Development* **138**, 2741-2749. doi:10.1242/dev.064402
Cheung, D., Miles, C., Kreitman, M. and Ma, J. (2014). Adaptation of the length scale and amplitude of the Bicoid gradient profile to achieve robust patterning in abnormally large Drosophila melanogaster embryos. *Development* **141**, 124-135. doi:10.1242/dev.098640
Chiang, C., Litingtung, Y., Harris, M. P., Simandl, B. K., Li, Y., Beachy, P. A. and Fallon, J. F. (2001). Manifestation of the limb prepattern: limb development in the absence of sonic hedgehog function. *Dev. Biol.* **236**, 421-435. doi:10.1006/dbio.2001.0346
Collins, Z. M., Ishimatsu, K., Tsai, T. Y. C. and Megason, S. G. (2019). A Scube2-Shh feedback loop links morphogen release to morphogen signaling to enable scale invariant patterning of the ventral neural tube. *BioRxiv*.
Cooke, J. (1975). Control of somite number during morphogenesis of a vertebrate, Xenopus laevis. *Nature* **254**, 196-199. doi:10.1038/254196a0
Cooke, J. and Zeeman, E. C. (1976). A clock and wavefront model for control of the number of repeated structures during animal morphogenesis. *J. Theor. Biol.* **58**, 455-476. doi:10.1016/S0022-5193(76)80131-2
Crick, F. (1970). Diffusion in embryogenesis. *Nature* **225**, 420-422. doi:10.1038/225420a0
Dalq, A. (1938). *Form and Causality in Early Development*. Cambridge: Cambridge University Press.
Day, S. J. and Lawrence, P. A. (2000). Measuring dimensions: the regulation of size and shape. *Development* **127**, 2977-2987.
De Robertis, E. M. (2006). Spemann's organizer and self-regulation in amphibian embryos. *Nat. Rev. Mol. Cell Biol.* **7**, 296-302. doi:10.1038/nrm1855
Diaz-Cuadros, M., Wagner, D. E., Budjan, C., Hubaud, A., Touboul, J., Michaut, A., Al Tanoury, Z., Yoshioka-Kobayashi, K., Niino, Y., Kageyama, R., et al. (2019). In vitro characterization of the human segmentation clock. *BioRxiv*.
Driesch, H. (1892). Entwicklungsmechanische Studien: I. Der Werth der beiden ersten Furchungszellen in der Echinodermenentwicklung. Experimentelle Erzeugung von Theil- und Doppelbildungen. *Z. Wiss. Zool.* **53**, 160-184.
Dubrulle, J., Jordan, B. M., Akhmetova, L., Farrell, J. A., Kim, S. H., Solnica-Krezel, L. and Schier, A. F. (2015). Response to Nodal morphogen gradient is determined by the kinetics of target gene induction. *eLife* **4**, e05042. doi:10.7554/eLife.05042
Fried, P. and Iber, D. (2014). Dynamic scaling of morphogen gradients on growing domains. *Nat. Commun.* **5**, 5077. doi:10.1038/ncomms6077
Galliot, B. (2013). Injury-induced asymmetric cell death as a driving force for head regeneration in Hydra. *Dev. Genes Evol.* **223**, 39-52. doi:10.1007/s00427-012-0411-y
Gierer, A. and Meinhardt, H. (1972). A theory of biological pattern formation. *Kybernetik* **12**, 30-39. doi:10.1007/BF00289234
Gomez, C., Özbudak, E. M., Wunderlich, J., Baumann, D., Lewis, J. and Pourquié, O. (2008). Control of segment number in vertebrate embryos. *Nature* **454**, 335-339. doi:10.1038/nature07020
Gregor, T., Bialek, W., de Ruyter van Steveninck, R. R., Tank, D. W. and Wieschaus, E. F. (2005). Diffusion and scaling during early embryonic pattern formation. *Proc. Natl. Acad. Sci. USA* **102**, 18403-18407. doi:10.1073/pnas.0509483102
Gregor, T., McGregor, A. P. and Wieschaus, E. F. (2008). Shape and function of the Bicoid morphogen gradient in dipteran species with different sized embryos. *Dev. Biol.* **316**, 350-358. doi:10.1016/j.ydbio.2008.01.039
Gufler, S., Artes, B., Bielen, H., Krainer, I., Eder, M.-K., Falschlunger, J., Bollmann, A., Ostermann, T., Valovka, T., Hartl, M., et al. (2018). β-Catenin acts in a position-independent regeneration response in the simple eumetazoan Hydra. *Dev. Biol.* **433**, 310-323. doi:10.1016/j.ydbio.2017.09.005
Gurley, K. A., Rink, J. C. and Sanchez Alvarado, A. (2008). β-Catenin defines head versus tail identity during planarian regeneration and homeostasis. *Science* **319**, 323-327. doi:10.1126/science.1150029
Gurley, K. A., Elliott, S. A., Simakov, O., Schmidt, H. A., Holstein, T. W. and Sanchez Alvarado, A. (2010). Expression of secreted Wnt pathway components reveals unexpected complexity of the planarian amputation response. *Dev. Biol.* **347**, 24-39. doi:10.1016/j.ydbio.2010.08.007
Hamaratoglu, F., de Lachapelle, A. M., Pyrowolakis, G., Bergmann, S. and Affolter, M. (2011). Dpp signaling activity requires Pentagone to scale with tissue size in the growing Drosophila wing imaginal disc. *PLoS Biol.* **9**, e1001182. doi:10.1371/journal.pbio.1001182
Harima, Y., Takashima, Y., Ueda, Y., Ohtsuka, T. and Kageyama, R. (2013). Accelerating the tempo of the segmentation clock by reducing the number of introns in the Hes7 gene. *Cell Rep.* **3**, 1-7. doi:10.1016/j.celrep.2012.11.012
Harmansa, S., Hamaratoglu, F., Affolter, M. and Caussinus, E. (2015). Dpp spreading is required for medial but not for lateral wing disc growth. *Nature* **527**, 317-322. doi:10.1038/nature15712
He, F., Wen, Y., Deng, J., Lin, X., Lu, L. J., Jiao, R. and Ma, J. (2008). Probing intrinsic properties of a robust morphogen gradient in Drosophila. *Dev. Cell* **15**, 558-567. doi:10.1016/j.devcel.2008.09.004
Herrgen, L., Ares, S., Morelli, L. G., Schröter, C., Jülicher, F. and Oates, A. C. (2010). Intercellular coupling regulates the period of the segmentation clock. *Curr. Biol.* **20**, 1244-1253. doi:10.1016/j.cub.2010.06.034
Hertwig, O. (1890). *Experimentelle Studien am thierischen Ei, vor, während und nach Befruchtung*. Jena: Fischer.
Hertwig, O. (1893). Ueber den Werth der ersten Furchungszellen für die Organbildung des Embryo. Experimentelle Studien am Frosch- und Tritonei. *Arch. Mikrosk. Anat.* **42**, 662-807. doi:10.1007/BF02976796
Hertwig, O. and Hertwig, R. (1887). *Über den Befruchtungs- und Teilungsvorgang des tierischen Eies unter dem Einfluss äußerer Agentien*. Jena: Fischer.
His, W. (1874). Princip der organbildenden Keimbezirke, dorsale und ventrale Flächen der Embryonalanlage und deren Sonderung; vorderes und hinteres Körperende; allgemeine Topographie der Keimbezirke. In *Unsere Körperform und das physiologische Problem ihrer Entstehung – Briefe an einen befreundeten Naturforscher*, pp. 18-31. Leipzig: F. C. W. Vogel.
Hoadley, L. (1928). On the localization of developmental potencies in the embryo of fundulus heteroclitus. *J. Exp. Zool.* **52**, 7-44. doi:10.1002/jez.1400520103
Hobmayer, B., Rentzsch, F., Kuhn, K., Happel, C. M., von Laue, C. C., Snyder, P., Rothbächer, U. and Holstein, T. W. (2000). WNT signalling molecules act in axis formation in the diploblastic metazoan Hydra. *Nature* **407**, 186-189. doi:10.1038/35025063
Holtfreter, J. (1938). Differenzierungspotenzen isolierter Teile der Urodelengastrula. *Wilhelm Roux Arch. Entwicklungsmech. Org.* **138**, 522-656. doi:10.1007/BF00573814
Houchmandzadeh, B., Wieschaus, E. and Leibler, S. (2005). Precise domain specification in the developing Drosophila embryo. *Phys. Rev. E Stat. Nonlin. Soft Matter Phys.* **72**, 061920. doi:10.1103/PhysRevE.72.061920
Huang, Y. and Umulis, D. M. (2019). Scale invariance of BMP signaling gradients in zebrafish. *Sci. Rep.* **9**, 5440. doi:10.1038/s41598-019-41840-8
Hufnagel, L., Teleman, A. A., Rouault, H., Cohen, S. M. and Shraiman, B. I. (2007). On the mechanism of wing size determination in fly development. *Proc. Natl. Acad. Sci. USA* **104**, 3835-3840. doi:10.1073/pnas.0607134104
Iglesias, M., Gomez-Skarmeta, J. L., Salo, E. and Adell, T. (2008). Silencing of Smed-betacatenin1 generates radial-like hypercephalized planarians. *Development* **135**, 1215-1221. doi:10.1242/dev.020289
Inomata, H. (2017). Scaling of pattern formations and morphogen gradients. *Dev. Growth Differ.* **59**, 41-51. doi:10.1111/dgd.12337
Inomata, H., Shibata, T., Haraguchi, T. and Sasai, Y. (2013). Scaling of dorsal-ventral patterning by embryo size-dependent degradation of Spemann's organizer signals. *Cell* **153**, 1296-1311. doi:10.1016/j.cell.2013.05.004
Ishihara, K. and Tanaka, E. M. (2018). Spontaneous symmetry breaking and pattern formation of organoids. *Curr. Opin. Syst. Biol.* **11**, 123-128. doi:10.1016/j.coisb.2018.06.002
Ishimatsu, K., Hiscock, T. W., Collins, Z. M., Sari, D. W. K., Lischer, K., Richmond, D. L., Bessho, Y., Matsui, T. and Megason, S. G. (2018). Size-reduced embryos reveal a gradient scaling-based mechanism for zebrafish somite formation. *Development* **145**, dev161257. doi:10.1242/dev.161257
Ishimatsu, K., Cha, A., Collins, Z. M. and Megason, S. G. (2019). Surgical size reduction of zebrafish for the study of embryonic pattern scaling. *J. Vis. Exp.* **147**, e59434. doi:10.3791/59434

Iten, L. E. and Bryant, S. V. (1975). The interaction between the blastema and stump in the establishment of the anterior-posterior and proximal-distal organization of the limb regenerate. *Dev. Biol.* **44**, 119-147. doi:10.1016/0012-1606(75)90381-4
Ivankovic, M., Haneckova, R., Thommen, A., Grohme, M. A., Vila-Farré, M., Werner, S. and Rink, J. C. (2019). Model systems for regeneration: planarians. *Development* **146**, dev167684. doi:10.1242/dev.167684
Joven, A., Elewa, A. and Simon, A. (2019). Model systems for regeneration: salamanders. *Development* **146**, dev167700. doi:10.1242/dev.167700
Kawakami, Y., Rodriguez Esteban, C., Raya, M., Kawakami, H., Marti, M., Dubova, I. and Izpisua Belmonte, J. C. (2006). Wnt/beta-catenin signaling regulates vertebrate limb regeneration. *Genes Dev.* **20**, 3232-3237. doi:10.1101/gad.1475106
Kicheva, A., Bollenbach, T., Ribeiro, A., Valle, H. P., Lovell-Badge, R., Episkopou, V. and Briscoe, J. (2014). Coordination of progenitor specification and growth in mouse and chick spinal cord. *Science* **345**, 1254927. doi:10.1126/science.1254927
Kragl, M., Knapp, D., Nacu, E., Khattak, S., Maden, M., Epperlein, H. H. and Tanaka, E. M. (2009). Cells keep a memory of their tissue origin during axolotl limb regeneration. *Nature* **460**, 60-65. doi:10.1038/nature08152
Landge, A., Jordan, B. M., Diego, X. and Müller, P. (2019). Pattern formation mechanisms of self-organizing reaction-diffusion systems. *Dev. Biol.* (in press).
Lauschke, V. M., Tsiairis, C. D., François, P. and Aulehla, A. (2013). Scaling of embryonic patterning based on phase-gradient encoding. *Nature* **493**, 101-105. doi:10.1038/nature11804
Lawrence, P. A. (1966). Gradients in the insect segment: the orientation of hairs in the milkweed bug Oncopeltus fasciatus. *J. Exp. Biol.* **44**.
Liem, K. F., Jr., Tremml, G. and Jessell, T. M. (1997). A role for the roof plate and its resident TGFβ-related proteins in neuronal patterning in the dorsal spinal cord. *Cell* **91**, 127-138. doi:10.1016/S0092-8674(01)80015-5
Liem, K. F., Jr., Jessell, T. M. and Briscoe, J. (2000). Regulation of the neural patterning activity of sonic hedgehog by secreted BMP inhibitors expressed by notochord and somites. *Development* **127**, 4855-4866.
MacWilliams, H. K. (1983). Hydra transplantation phenomena and the mechanism of Hydra head regeneration: II. Properties of the head activation. *Dev. Biol.* **96**, 239-257. doi:10.1016/0012-1606(83)90325-1
Mangold, O. (1960). Molchlarven ohne Zentralnervensystem und ohne Ektomesoderm. *Roux Arch. Entwicklungsmech.* **152**, 725-769. doi:10.1007/BF00581847
Marcon, L., Diego, X., Sharpe, J. and Müller, P. (2016). High-throughput mathematical analysis identifies Turing networks for patterning with equally diffusing signals. *eLife* **5**, e14022. doi:10.7554/eLife.14022
Matsuda, M., Yamanaka, Y., Uemura, M., Osawa, M., Saito, M. K., Nagahashi, A., Nishio, M., Guo, L., Ikegawa, S., Sakurai, S., et al. (2019). Modeling the human segmentation clock with pluripotent stem cells. *BioRxiv*.
McCusker, C., Lehrberg, J. and Gardiner, D. (2014). Position-specific induction of ectopic limbs in non-regenerating blastemas on axolotl forelimbs. *Regeneration (Oxf)* **1**, 27-34. doi:10.1002/reg2.10
McHale, P., Rappel, W. J. and Levine, H. (2006). Embryonic pattern scaling achieved by oppositely directed morphogen gradients. *Phys. Biol.* **3**, 107-120. doi:10.1088/1478-3975/3/2/003
Meinhardt, H. (2009). Models for the generation and interpretation of gradients. *Cold Spring Harb. Perspect. Biol.* **1**, a001362. doi:10.1101/cshperspect.a001362
Morgan, T. H. (1895). Half embryos and whole embryos from one of the first two blastomeres. *Anat. Anz.* **10**, 623-685.
Morgan, T. H. (1896). The number of cells in larvae from isolated blastomeres of Amphioxus. *Arch. Entwicklungsmech. Org.* **3**, 269-294. doi:10.1007/BF02152851
Morgan, T. H. (1898). Experimental studies of the regeneration of Planaria maculata. *Roux's Arch. Dev. Biol.* **7**, 364-397. doi:10.1007/BF02161491
Morgan, T. H. (1901). *Regeneration*. New York: Macmillan.
Morgan, T. H. (1924). Two embryos from one egg. *Sci. Mon.* **18**, 529-546.
Mori, Y., Jilkine, A. and Edelstein-Keshet, L. (2008). Wave-pinning and cell polarity from a bistable reaction-diffusion system. *Biophys. J.* **94**, 3684-3697. doi:10.1529/biophysj.107.120824
Moriyama, Y. and De Robertis, E. M. (2018). Embryonic regeneration by relocalization of the Spemann organizer during twinning in Xenopus. *Proc. Natl. Acad. Sci. USA* **115**, E4815-E4822. doi:10.1073/pnas.1802749115
Müller, P. and Nüsslein-Volhard, C. (2016). Obituary: Hans Meinhardt (1938-2016). *Development* **143**, 1231-1233. doi:10.1242/dev.137414
Müller, P. and Schier, A. F. (2011). Extracellular movement of signaling molecules. *Dev. Cell* **21**, 145-158. doi:10.1016/j.devcel.2011.06.001
Müller, P., Rogers, K. W., Jordan, B. M., Lee, J. S., Robson, D., Ramanathan, S. and Schier, A. F. (2012). Differential diffusivity of Nodal and Lefty underlies a reaction-diffusion patterning system. *Science* **336**, 721-724. doi:10.1126/science.1221920
Müller, P., Rogers, K. W., Yu, S. R., Brand, M. and Schier, A. F. (2013). Morphogen transport. *Development* **140**, 1621-1638. doi:10.1242/dev.083519
Murray, J. D. (2013). *Mathematical Biology II: Spatial Models and Biomedical Applications*. New York: Springer.
Nacu, E., Glausch, M., Le, H. Q., Damanik, F. F., Schuez, M., Knapp, D., Khattak, S., Richter, T. and Tanaka, E. M. (2013). Connective tissue cells, but not muscle cells, are involved in establishing the proximo-distal outcome of limb regeneration in the axolotl. *Development* **140**, 513-518. doi:10.1242/dev.081752
Nacu, E., Gromberg, E., Oliveira, C. R., Drechsel, D. and Tanaka, E. M. (2016). FGF8 and SHH substitute for anterior-posterior tissue interactions to induce limb regeneration. *Nature* **533**, 407-410. doi:10.1038/nature17972
Nakajima, T., Shibata, M., Nishio, M., Nagata, S., Alev, C., Sakurai, H., Toguchida, J. and Ikeya, M. (2018). Modeling human somite development and fibrodysplasia ossificans progressiva with induced pluripotent stem cells. *Development* **145**, dev165431. doi:10.1242/dev.165431
Nesterenko, A. M. and Zaraisky, A. G. (2019). The mechanisms of embryonic scaling. *Russ. J. Dev. Biol.* **50**, 95-101. doi:10.1134/S1062360419030044
Nicholas, J. S. and Oppenheimer, J. M. (1942). Regulation and reconstitution in Fundulus. *J. Exp. Zool.* **90**, 127-157. doi:10.1002/jez.1400900108
Oates, A. C., Morelli, L. G. and Ares, S. (2012). Patterning embryos with oscillations: structure, function and dynamics of the vertebrate segmentation clock. *Development* **139**, 625-639. doi:10.1242/dev.063735
Othmer, H. G. and Pate, E. (1980). Scale-invariance in reaction-diffusion models of spatial pattern formation. *Proc. Natl. Acad. Sci. USA* **77**, 4180-4184. doi:10.1073/pnas.77.7.4180
Palmeirim, I., Henrique, D., Ish-Horowicz, D. and Pourquié, O. (1997). Avian hairy gene expression identifies a molecular clock linked to vertebrate segmentation and somitogenesis. *Cell* **91**, 639-648. doi:10.1016/S0092-8674(00)80451-1
Pate, E. and Othmer, H. G. (1984). Applications of a model for scale-invariant pattern formation in developing systems. *Differentiation* **28**, 1-8. doi:10.1111/j.1432-0436.1984.tb00259.x
Pescitelli, M. J. and Stocum, D. L. (1980). The origin of skeletal structures during intercalary regeneration of larval Ambystoma limbs. *Dev. Biol.* **79**, 255-275. doi:10.1016/0012-1606(80)90115-3
Petersen, C. P. and Reddien, P. W. (2008). Smed-betacatenin-1 is required for anteroposterior blastema polarity in planarian regeneration. *Science* **319**, 327-330. doi:10.1126/science.1149943
Petersen, C. P. and Reddien, P. W. (2009). A wound-induced Wnt expression program controls planarian regeneration polarity. *Proc. Natl. Acad. Sci. USA* **106**, 17061-17066. doi:10.1073/pnas.0906823106
Petersen, C. P. and Reddien, P. W. (2011). Polarized notum activation at wounds inhibits Wnt function to promote planarian head regeneration. *Science* **332**, 852-855. doi:10.1126/science.1202143
Pietak, A., Bischof, J., LaPalme, J., Morokuma, J. and Levin, M. (2019). Neural control of body-plan axis in regenerating planaria. *PLoS Comput. Biol.* **15**, e1006904. doi:10.1371/journal.pcbi.1006904
Pomreinke, A. P., Soh, G. H., Rogers, K. W., Bergmann, J. K., Bläßle, A. J. and Müller, P. (2017). Dynamics of BMP signaling and distribution during zebrafish dorsal-ventral patterning. *eLife* **6**, e25861. doi:10.7554/eLife.25861
Rahimi, N., Averbukh, I., Haskel-Ittah, M., Degani, N., Schejter, E. D., Barkai, N. and Shilo, B. Z. (2016). A WntD-dependent integral feedback loop attenuates variability in Drosophila Toll signaling. *Dev. Cell* **36**, 401-414. doi:10.1016/j.devcel.2016.01.023
Rasolonjanahary, M. and Vasiev, B. (2016). Scaling of morphogenetic patterns in reaction-diffusion systems. *J. Theor. Biol.* **404**, 109-119. doi:10.1016/j.jtbi.2016.05.035
Rasolonjanahary, M. and Vasiev, B. (2018). Scaling of morphogenetic patterns. *Methods Mol. Biol.* **1863**, 263-280. doi:10.1007/978-1-4939-8772-6_15
Recho, P., Hallou, A. and Hannezo, E. (2019). Theory of mechanochemical patterning in biphasic biological tissues. *Proc. Natl. Acad. Sci. USA* **116**, 5344-5349. doi:10.1073/pnas.1813255116
Reddien, P. W. (2018). The cellular and molecular basis for planarian regeneration. *Cell* **175**, 327-345. doi:10.1016/j.cell.2018.09.021
Reversade, B. and De Robertis, E. M. (2005). Regulation of ADMP and BMP2/4/7 at opposite embryonic poles generates a self-regulating morphogenetic field. *Cell* **123**, 1147-1160. doi:10.1016/j.cell.2005.08.047
Rink, J. C., Gurley, K. A., Elliott, S. A. and Sanchez Alvarado, A. (2009). Planarian Hh signaling regulates regeneration polarity and links Hh pathway evolution to cilia. *Science* **326**, 1406-1410. doi:10.1126/science.1178712
Roelink, H., Porter, J. A., Chiang, C., Tanabe, Y., Chang, D. T., Beachy, P. A. and Jessell, T. M. (1995). Floor plate and motor neuron induction by different concentrations of the amino-terminal cleavage product of sonic hedgehog autoproteolysis. *Cell* **81**, 445-455. doi:10.1016/0092-8674(95)90397-6
Roensch, K., Tazaki, A., Chara, O. and Tanaka, E. M. (2013). Progressive specification rather than intercalation of segments during limb regeneration. *Science* **342**, 1375-1379. doi:10.1126/science.1241796
Rogers, K. W. and Müller, P. (2019). Nodal and BMP dispersal during early zebrafish development. *Dev. Biol.* **447**, 14-23. doi:10.1016/j.ydbio.2018.04.002
Rogers, K. W. and Schier, A. F. (2011). Morphogen gradients: from generation to interpretation. *Annu. Rev. Cell Dev. Biol.* **27**, 377-407. doi:10.1146/annurev-cellbio-092910-154148
Rogers, K. W., Lord, N. D., Gagnon, J. A., Pauli, A., Zimmerman, S., Aksel, D. C., Reyon, D., Tsai, S. Q., Joung, J. K. and Schier, A. F. (2017). Nodal patterning without Lefty inhibitory feedback is functional but fragile. *eLife* **6**, e28785. doi:10.7554/eLife.28785
Rogulja, D. and Irvine, K. D. (2005). Regulation of cell proliferation by a morphogen gradient. *Cell* **123**, 449-461. doi:10.1016/j.cell.2005.08.030

Romanova-Michaelides, M., Aguilar-Hidalgo, D., Jülicher, F. and González-Gaitán, M. (2015). The wing and the eye: a parsimonious theory for scaling and growth control? *Wiley Interdiscip. Rev. Dev. Biol.* **4**, 591-608. doi:10.1002/wdev.195

Roux, W. (1885). Beiträge zur Entwicklungsmechanik des Embryo. Nr. I. Einleitung und Orientierung über einige Probleme der embryonalen Entwicklung. *Z. Biol.* **21**, 411-452.

Roux, W. (1894). Die Methoden zur Erzeugung halber Froschembryonen und zum Nachweis der Beziehung der ersten Furchungsebenen des Froscheies zur Medianebene des Embryo. *Anat. Anz.* **9**, 248-263.

Ruud, G. and Spemann, H. (1922). Die Entwicklung isolierter dorsaler und lateraler Gastrulahälften von Triton taeniatus und alpestris, ihre Regulation und Postgeneration. *Arch. Entwicklungsmech. Org.* **52**, 95-166. doi:10.1007/BF02137446

Sander, K. (1959). Analyse des ooplasmatischen Reaktionssystems von Euscelis plebejus Fall. (Cicadina) durch Isolieren und Kombinieren von Keimteilen. *Wilhelm Roux' Arch. Entwicklungsmech.* **151**, 430-497. doi:10.1007/BF00573355

Saxena, A., Towers, M. and Cooper, K. L. (2016). The origins, scaling and loss of tetrapod digits. *Philos. Trans. R. Soc. Lond. B Biol. Sci.* **372**, 20150482. doi:10.1098/rstb.2015.0482

Scherz, P. J., Harfe, B. D., McMahon, A. P. and Tabin, C. J. (2004). The limb bud Shh-Fgf feedback loop is terminated by expansion of former ZPA cells. *Science* **305**, 396-399. doi:10.1126/science.1096966

Schier, A. F. (2009). Nodal morphogens. *Cold Spring Harb. Perspect. Biol.* **1**, a003459. doi:10.1101/cshperspect.a003459

Schröter, C. and Oates, A. C. (2010). Segment number and axial identity in a segmentation clock period mutant. *Curr. Biol.* **20**, 1254-1258. doi:10.1016/j.cub.2010.05.071

Schröter, C., Herrgen, L., Cardona, A., Brouhard, G. J., Feldman, B. and Oates, A. C. (2008). Dynamics of zebrafish somitogenesis. *Dev. Dyn.* **237**, 545-553. doi:10.1002/dvdy.21458

Shilo, B. Z. and Barkai, N. (2017). Buffering global variability of morphogen gradients. *Dev. Cell* **40**, 429-438. doi:10.1016/j.devcel.2016.12.012

Spemann, H. (1903). Entwickelungsphysiologische Studien am Triton-Ei. *Arch. Entwicklungsmech. Org.* **16**, 551-631. doi:10.1007/BF02301267

Spemann, H. (1938). *Embryonic Development and Induction*. New Haven: Yale Univ.

Spemann, H. and Mangold, H. (1924). Induction of embryonic primordia by implantation of organizers from a different species. 1923. *Int. J. Dev. Biol.* **45**, 13-38.

Stückemann, T., Cleland, J. P., Werner, S., Thi-Kim Vu, H., Bayersdorf, R., Liu, S. Y., Friedrich, B., Jülicher, F. and Rink, J. C. (2017). Antagonistic self-organizing patterning systems control maintenance and regeneration of the anteroposterior axis in planarians. *Dev. Cell* **40**, 248-263.e4. doi:10.1016/j.devcel.2016.12.024

Stumpf, H. F. (1966). Mechanism by which cells estimate their location within the body. *Nature* **212**, 430-431. doi:10.1038/212430a0

Tanaka, E. M. (2016). The molecular and cellular choreography of appendage regeneration. *Cell* **165**, 1598-1608. doi:10.1016/j.cell.2016.05.038

Tanaka, E. M. (2018). Regenerating tissues. *Science* **360**, 374-375. doi:10.1126/science.aat4588

Tasaki, J., Shibata, N., Nishimura, O., Itomi, K., Tabata, Y., Son, F., Suzuki, N., Araki, R., Abe, M., Agata, K. et al. (2011). ERK signaling controls blastema cell differentiation during planarian regeneration. *Development* **138**, 2417-2427. doi:10.1242/dev.060764

Turing, A. M. (1952). The chemical basis of morphogenesis. *Philos. Trans. R. Soc. B Biol. Sci.* **237**, 19520012. doi:10.1098/rstb.1952.0012

Umesono, Y., Tasaki, J., Nishimura, Y., Hrouda, M., Kawaguchi, E., Yazawa, S., Nishimura, O., Hosoda, K., Inoue, T. and Agata, K. (2013). The molecular logic for planarian regeneration along the anterior-posterior axis. *Nature* **500**, 73-76. doi:10.1038/nature12359

Umulis, D. M. and Othmer, H. G. (2013). Mechanisms of scaling in pattern formation. *Development* **140**, 4830-4843. doi:10.1242/dev.100511

Uygur, A., Young, J., Huycke, T. R., Koska, M., Briscoe, J. and Tabin, C. J. (2016). Scaling pattern to variations in size during development of the vertebrate neural tube. *Dev. Cell* **37**, 127-135. doi:10.1016/j.devcel.2016.03.024

Vincent, C. D., Rost, F., Masselink, W., Brusch, L. and Tanaka, E. M. (2015). Cellular dynamics underlying regeneration of appropriate segment number during axolotl tail regeneration. *BMC Dev. Biol.* **15**, 48. doi:10.1186/s12861-015-0098-1

Vogg, M. C., Beccari, L., Iglesias Ollé, L., Rampon, C., Vriz, S., Perruchoud, C., Wenger, Y. and Galliot, B. (2019a). An evolutionarily-conserved Wnt3/beta-catenin/Sp5 feedback loop restricts head organizer activity in Hydra. *Nat. Commun.* **10**, 312. doi:10.1038/s41467-018-08242-2

Vogg, M. C., Galliot, B. and Tsiairis, C. D. (2019b). Model systems for regeneration: Hydra. *Development* **146**, dev177212. doi:10.1242/dev.177212

Vogt, W. and Bruns, E. (1930). Experimente über das Regulationsvermögen der Blastula von Triton taeniatus und Bombinator pachypus. *Roux Arch. Entwicklungsmech.* **122**, 667-669. doi:10.1007/BF00573597

Wartlick, O., Kicheva, A. and González-Gaitán, M. (2009). Morphogen gradient formation. *Cold Spring Harb. Perspect. Biol.* **1**, a001255. doi:10.1101/cshperspect.a001255

Wartlick, O., Mumcu, P., Kicheva, A., Bittig, T., Seum, C., Jülicher, F. and González-Gaitán, M. (2011). Dynamics of Dpp signaling and proliferation control. *Science* **331**, 1154-1159. doi:10.1126/science.1200037

Wenemoser, D., Lapan, S. W., Wilkinson, A. W., Bell, G. W. and Reddien, P. W. (2012). A molecular wound response program associated with regeneration initiation in planarians. *Genes Dev.* **26**, 988-1002. doi:10.1101/gad.187377.112

Werner, S., Stückemann, T., Beirán Amigo, M., Rink, J. C., Jülicher, F. and Friedrich, B. M. (2015). Scaling and regeneration of self-organized patterns. *Phys. Rev. Lett.* **114**, 138101. doi:10.1103/PhysRevLett.114.138101

Wilby, O. K. and Webster, G. (1970). Experimental studies on axial polarity in hydra. *J. Embryol. Exp. Morphol.* **24**, 595-613.

Wilson, E. B. (1893). Amphioxus, and the mosaic theory of development. *J. Morphol.* **8**, 579-638. doi:10.1002/jmor.1050080306

Witchley, J. N., Mayer, M., Wagner, D. E., Owen, J. H. and Reddien, P. W. (2013). Muscle cells provide instructions for planarian regeneration. *Cell Rep.* **4**, 633-641. doi:10.1016/j.celrep.2013.07.022

Wolpert, L. (1968). The French flag problem: a contribution to the discussion on pattern development and regulation. In *Towards a Theoretical Biology* (ed. C. H. Waddington), pp. 125-133. Ediburgh: Edinburgh University Press.

Wolpert, L. (1969). Positional information and the spatial pattern of cellular differentiation. *J. Theor. Biol.* **25**, 1-47. doi:10.1016/S0022-5193(69)80016-0

Wurtzel, O., Cote, L. E., Poirier, A., Satija, R., Regev, A. and Reddien, P. W. (2015). A generic and cell-type-specific wound response precedes regeneration in planarians. *Dev. Cell* **35**, 632-645. doi:10.1016/j.devcel.2015.11.004

Yazawa, S., Umesono, Y., Hayashi, T., Tarui, H. and Agata, K. (2009). Planarian hedgehog/patched establishes anterior-posterior polarity by regulating Wnt signaling. *Proc. Natl. Acad. Sci. USA* **106**, 22329-22334. doi:10.1073/pnas.0907464106

Zagorski, M., Tabata, Y., Brandenberg, N., Lutolf, M. P., Tkačik, G., Bollenbach, T., Briscoe, J. and Kicheva, A. (2017). Decoding of position in the developing neural tube from antiparallel morphogen gradients. *Science* **356**, 1379-1383. doi:10.1126/science.aam5887

Zinski, J., Bu, Y., Wang, X., Dou, W., Umulis, D. and Mullins, M. C. (2017). Systems biology derived source-sink mechanism of BMP gradient formation. *eLife* **6**, e22199. doi:10.7554/eLife.22199

Zinski, J., Tajer, B. and Mullins, M. C. (2018). TGF-β family signaling in early vertebrate development. *Cold Spring Harb. Perspect. Biol.* **10**, a033274. doi:10.1101/cshperspect.a033274